Progress in observations and simulations of global change in the upper atmosphere

Liying Qian,[1] Jan Laštovička,[2] Raymond G. Roble,[1] and Stanley C. Solomon[1]

Received 24 November 2010; revised 14 January 2011; accepted 31 January 2011; published 13 April 2011.

[1] Anthropogenic increases of greenhouse gases warm the troposphere but have a cooling effect in the middle and upper atmosphere. The steady increase of CO_2 is the dominant cause of upper atmosphere trends; other drivers are long-term changes of radiatively active trace gases such as CH_4, O_3, and H_2O, secular change of solar and geomagnetic activity, and evolution of the Earth's magnetic field. Observational and model studies have confirmed that in the past several decades, global cooling has occurred in the mesosphere and thermosphere; the cooling and contraction of the upper atmosphere has lowered the ionosphere and increased electron density in the E and F_1 regions. Trends of other parameters, including the F_2 region, mesospheric clouds, and mesopause wave activity, have been more controversial. Modeling investigations have demonstrated that both greenhouse gas forcing and secular change of the Earth's magnetic field can cause regional, diurnal, and seasonal variability of trends in F_2 region density and height, which may contribute to discrepancies regarding ionospheric trends. Recent studies also may have reconciled discrepancies between space-based and ground-based observations of mesospheric clouds: both types of observations do not find statistically significant trends in the ~54°N–~64°N latitude region, but space-based observations indicate that clouds may be increasing in frequency at higher latitude. Limited observational studies have suggested possible trends in wave activity. Changes in atmospheric dynamics, both as a consequence of global change in the lower and middle atmosphere and as a possible driver of trends in the upper atmosphere, is one of the critical open questions regarding trends in the upper atmosphere and ionosphere.

Citation: Qian, L., J. Laštovička, R. G. Roble, and S. C. Solomon (2011), Progress in observations and simulations of global change in the upper atmosphere, *J. Geophys. Res.*, *116*, A00H03, doi:10.1029/2010JA016317.

1. Introduction

[2] Anthropogenic emissions of greenhouse gases influence the troposphere, its weather and climate, and are the primary cause of a substantial warming of the atmosphere near the surface during the past 50 years. These gases also influence the atmosphere at nearly all altitudes between the ground and the upper thermosphere, thus affecting not only life on the surface, but also space-based technological systems. Tropospheric climate is the most societally relevant component of global atmospheric change, but as the impact of trace gases on the Earth's ozone layer illustrates, changes at higher levels of the atmosphere can be important as well. In order to understand the full spectrum of human effects on the global system, it is necessary to obtain a complete understanding of atmospheric change throughout its vertical extent. The purpose of this paper is to provide an overview of the knowledge and understanding of long-term changes in the upper atmosphere (mesosphere and thermosphere) and ionosphere, with a particular focus on progress made in the last several years.

[3] The 0.6 K increase in global surface air temperature during the twentieth century [e.g., *Intergovernmental Panel on Climate Change* (*IPCC*), 2007] has been attributed predominantly to the increasing atmospheric concentration of greenhouse gases. However, greenhouse gases have an opposite, cooling effect in the upper atmosphere. These gases in the troposphere are optically thick to outgoing infrared radiation, which they both absorb and reemit back to the surface to produce the heating effect. In contrast, greenhouse gases in the much lower density upper atmosphere are optically thin to outgoing infrared radiation. In situ collisional excitation causes the loss of thermal energy through infrared radiation to space, while the absorption of radiation emanating from the lower atmosphere plays only a secondary role in the energy balance. The net result is that radiatively active greenhouse gases act as cooling agents at high altitude, and their increasing concentrations lower the temperature of the upper atmosphere. The combination of lower atmosphere heating and the upper atmosphere cooling is demonstrated

[1]High Altitude Observatory, National Center for Atmospheric Research, Boulder, Colorado, USA.
[2]Institute of Atmospheric Physics, ASCR, Prague, Czech Republic.

0148-0227/11/2010JA016317

by the much stronger greenhouse effect that is observed on Venus, where the high density of carbon dioxide results in a tropospheric temperature that is more than twice that of the Earth, but a thermosphere that is 4 to 5 times colder [e.g., *Bougher and Roble*, 1991].

[4] Long-term changes in the upper atmosphere and ionosphere have been of interest since *Roble and Dickinson* [1989] suggested that global cooling would occur in the upper atmosphere in conjunction with global warming in the troposphere due to the long-term increase of greenhouse gas concentrations, particularly carbon dioxide (CO_2). This effect of greenhouse gases has been referred to as "greenhouse cooling" [*Cicerone*, 1990]. Modeling studies by *Rishbeth* [1990] and *Rishbeth and Roble* [1992] broadened these results to the thermosphere-ionosphere system.

[5] The first observational results were by *Laštovička and Pancheva* [1991]. Subsequently, changes in thermospheric density have been detected and characterized. Since the global atmosphere is close to hydrostatic equilibrium, the height of a given pressure surface is determined by the average atmospheric temperature below. The cooling therefore results in thermal contraction of the upper atmosphere, and we may expect a significant decline in thermospheric density at fixed heights, which has been observed through the long-term effects of atmospheric drag on satellite orbits [e.g., *Keating et al.*, 2000; *Emmert et al.*, 2004, 2008; *Marcos et al.*, 2005]. These satellite drag observations have been the clearest confirmed detection of upper atmosphere global change. The cooling-related reduction of thermospheric density has practical importance due to its influence on satellite drag and the orbital lifetime of hazardous space debris.

[6] Determination of long-term changes in the upper atmosphere and ionosphere also has important scientific interest. It can facilitate monitoring of global change in the lower atmosphere since global change in the lower atmosphere and upper atmosphere/ionosphere are closely linked, and it can be easier to detect global changes in the upper atmosphere and ionosphere due to the larger signal-to-noise ratio [e.g., *Laštovička et al.*, 2006a]. Long-term changes and trends in the upper atmosphere have been studied much less extensively than those in the lower atmosphere, but the topic has grown over the past two decades into an active area of investigation. Significant additional progress has been made through both observational and modeling studies. These studies obtained long-term trends of mesospheric cooling [e.g., *Clemesha et al.*, 1992; *Beig et al.*, 2003], long-term decrease in height and increase in electron density in the ionosphere E and F_1 regions [e.g., *Bremer*, 1998; *Laštovička and Bremer*, 2004], and both positive and negative trends in the ionosphere F_2 region [e.g., *Danilov and Mikhailov*, 1999; *Laštovička et al.*, 2006b]. Most recent studies advanced our understanding of long-term trends in the ionosphere F_2 region [e.g., *Danilov*, 2009b; *Bencze*, 2009; *Qian et al.*, 2009], water vapor related phenomena [e.g., *Bremer et al.*, 2009b; *Lübken et al.*, 2009], mesosphere–lower thermosphere dynamics [e.g., *Merzlyakov et al.*, 2009; *Sridharan et al.*, 2010], as well as drivers of the long-term trends in the upper atmosphere and ionosphere [e.g., *Mikhailov*, 2006; *Akmaev et al.*, 2006; *Qian et al.*, 2006; *Cnossen and Richmond*, 2008; *Elias*, 2009].

[7] This paper will review the knowledge and understanding of long-term trends in the upper atmosphere and ionosphere with a focus on the recent progress. Section 2 gives a description of the expected trend scenario in the upper atmosphere and ionosphere. Sections 3, 4, and 5 discuss recent progresses in the ionosphere, mesosphere–lower thermosphere dynamics, and water vapor related phenomena, respectively. Section 6 addresses the drivers of trends in the upper atmosphere and ionosphere. Section 7 concludes the review and discusses directions for future investigations.

2. Trend Scenario

[8] Long-term data sets of mesospheric, thermospheric, and ionospheric parameters have been used to detect changes in the upper atmosphere and ionosphere. Mesospheric models, thermosphere/ionosphere models, and whole atmosphere models have been used to investigate these changes, and their forcing mechanisms. A global pattern of changes in the upper atmosphere and ionosphere has emerged through these observational and modeling studies [*Laštovička et al.*, 2008a; *Laštovička*, 2009] as summarized in Figure 1: temperature in the mesosphere and thermosphere has decreased, with larger decreases at higher altitude; temperature near the mesopause and in the lower thermosphere region has exhibited no significant change or even slight positive change; electron density in the E and F_1 regions has increased; the altitude of the E region ionosphere has decreased. These trends are consistent with modeling results, and with the hypothesis of global cooling and contracting of the upper atmosphere [e.g., *Rishbeth and Roble*, 1992; *Qian et al.*, 2009]. Trends of other parameters, such as in the F_2 region, polar mesospheric clouds (PMC) and noctilucent clouds (NLC), and wave activity in the mesopause region, have been more controversial. The dominant driver of these trends has been attributed to the increasing CO_2 cooling [*Laštovička et al.*, 2006a]. Other forcing mechanisms such as changes in other radiatively active trace gases (e.g., O_3 and H_2O) [e.g., *Akmaev et al.*, 2006], long-term change in geomagnetic activity [e.g., *Mikhailov*, 2002], and long-term change in the Earth's magnetic field [e.g., *Cnossen and Richmond*, 2008], also contributed.

[9] Figure 2 illustrates cooling and contraction of the upper atmosphere due to greenhouse gas forcing. Zonal mean and global mean changes of temperature and geopotential height are shown as a result of doubling of CO_2, under geomagnetic quiet and equinoctial conditions, simulated by the National Center for Atmospheric Research (NCAR) Thermosphere-Ionosphere-Mesosphere-Electrodynamics general circulation model (TIME-GCM) [*Roble and Ridley*, 1994]. For solar minimum conditions, cooling in the mesosphere is approximately −10 K; it increases to about −50 K in the upper thermosphere (Figures 2a and 2b). In the mesopause and lower thermosphere, there is an altitude region where there is no or very small positive change of the temperature (Figure 2a). Pressure surfaces decrease for several kilometers in the mesosphere and lower thermosphere, reaching up to ~−30 km in the upper thermosphere (Figures 2c and 2d). This cooling and contraction of the upper atmosphere depends on solar activity. Figure 2b shows a comparison of cooling for solar minimum and solar maximum conditions. Cooling in the thermosphere is much weaker for solar maximum conditions compared to solar minimum due to the changing relative importance of CO_2 cooling and nitric oxide (NO)

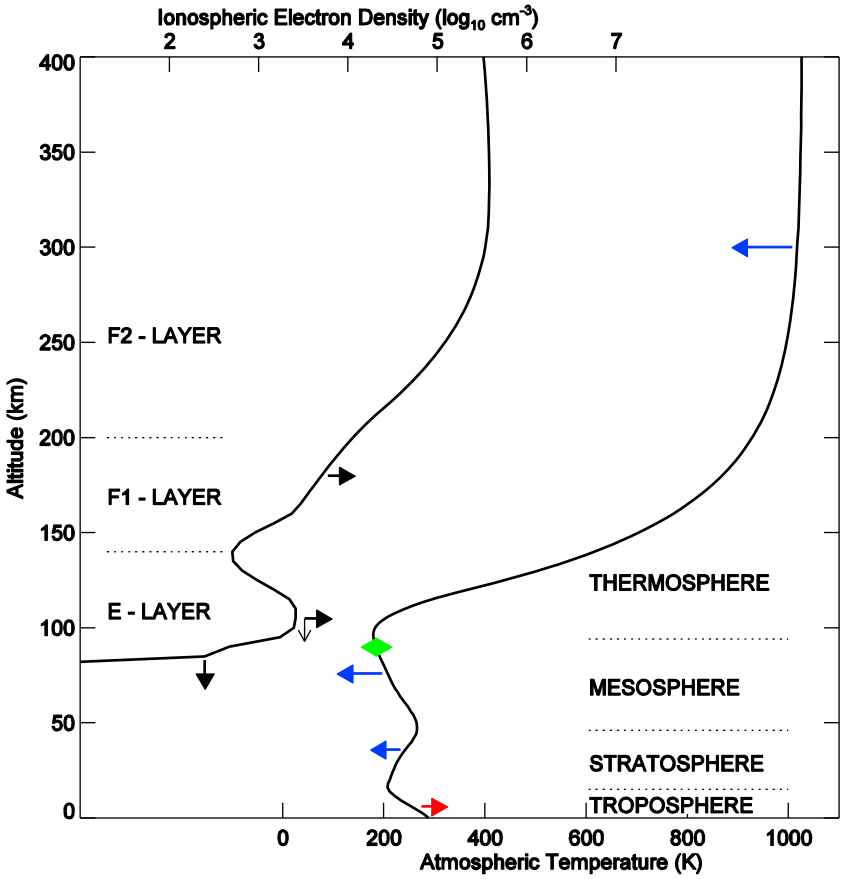

Figure 1. Trends in Earth's atmosphere. The atmospheric layers are defined by the temperature profile. The ionospheric layers are defined by the electron density profile (midnight at equator). Arrows indicate the direction of change: red, warming; blue, cooling; green, no change of temperature; black, changes in electron density (horizontal) and heights of ionospheric layers (vertical). From *Laštovička et al.* [2008a].

cooling under different solar activity conditions; this is discussed in more detail below. It is important to point out that the CO_2 cooling effect may not be linear, but may depend on the base CO_2 concentration. All modeling results from the NCAR models discussed in this paper used a base CO_2 concentration of 365 ppmv, representative of the year 2000. The doubling of CO_2 (730 ppmv) represents a projection of CO_2 concentration for year 2100 by the *IPCC* [2007]. CO_2 cooling depends on the collisional excitation rate between CO_2 and O. This collisional rate has a large uncertainty, ranging from $\sim 10^{-12}$ cm^3 s^{-1} to 6×10^{-12} cm^3 s^{-1} [e.g., *Shved et al.*, 1991; *Pollock et al.*, 1993; *Rodgers et al.*, 1992; *Sharma and Wintersteiner*, 1990]. In the NCAR models, the rate employed is 1.56×10^{-12} cm^3 s^{-1} for $T < 260$ K, 1.4×10^{-12} cm^3 s^{-1} for $T > 300$ K, and linear interpretation in between. In addition, NO infrared cooling at 5.3 μm is a significant component of the thermospheric energy balance, which will be discussed in section 6. Similarly, NO cooling depends on the collisional excitation rate between NO and O. Estimates of this rate range from $\sim 2.7 \times 10^{-11}$ cm^3 s^{-1} to 6.5×10^{-11} cm^3 s^{-1} [e.g., *Klein and Herron*, 1964; *Glänzer and Troe*, 1975; *Fernando and Smith*, 1979; *Sharma and Roble*, 2002]. In the NCAR models, it is set to 4.2×10^{-11} cm^3 s^{-1}.

[10] This trend scenario together with long-term trends in the stratosphere and troposphere shown in Figure 1 demonstrate that anthropogenic emissions of greenhouse gases influence the atmosphere at nearly all altitudes between the ground and space. Trends of mesospheric temperature have been detected through direct measurements by ground-based instruments and instruments carried by rocket sonde and satellites [e.g., *Bittner et al.*, 2002; *Golitsyn et al.*, 2000; *Lübken*, 2001; *Nielsen et al.*, 2002; *She et al.*, 2009]; or they have been inferred from ionospheric parameters or descending height trend of sodium emission layer [e.g., *Clemesha et al.*, 1992; *Semenov et al.*, 2002]. On the modeling side, *Roble and Dickinson* [1989] predicted a cooling of about −10K in the mesosphere from a doubling of CO_2 and CH_4. Subsequent modeling studies confirmed and elaborated on this work [e.g., *Akmaev and Fomichev*, 2000; *Fomichev et al.*, 2007; *Garcia et al.*, 2007; *Gruzdev and Brasseur*, 2005; *Schmidt et al.*, 2006]. *Beig et al.* [2003] conducted a comprehensive review of observational and modeling results. They concluded that overall, there is cooling in the order of −2 to −3 K/decade in the altitude region from 50 km to 80 km whereas there is no significant trend in the mesopause region from 80 km to 100 km; updating by *Beig* [2006] did not change these results.

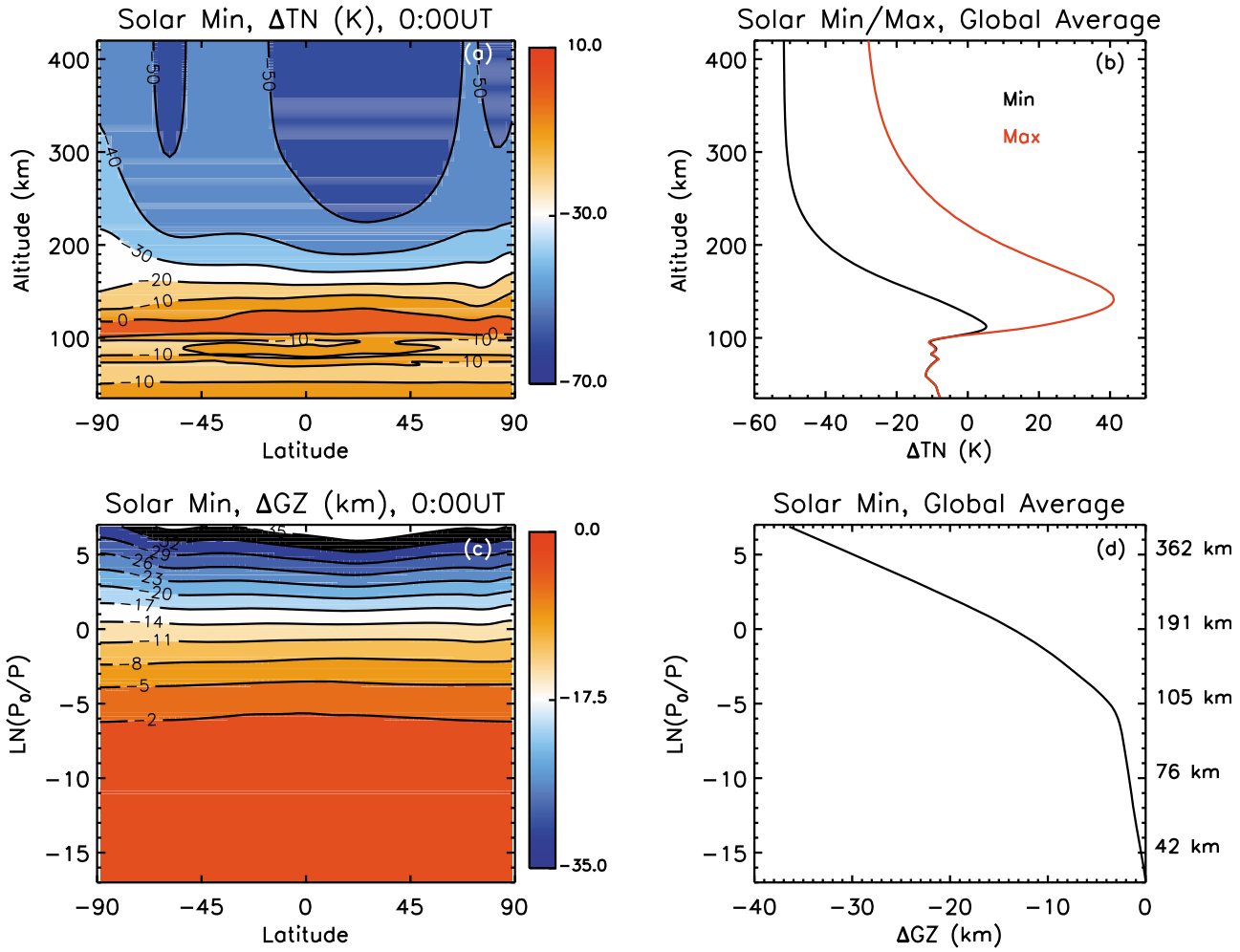

Figure 2. Changes (double CO_2–base CO_2) of temperature and geopotential height due to doubling of CO_2, under geomagnetic quiet and equinoctial conditions, at 0000 UT, simulated by the NCAR TIME-GCM. (a) Zonal mean temperature change for solar minimum condition; (b) global mean temperature change for solar minimum (black) and solar maximum (red) conditions; (c) zonal mean geopotential height change for solar minimum condition; and (d) global mean geopotential height change for solar minimum condition. $LN(P_0/P)$ is model pressure surface, where P is pressure at model surface and P_0 is a reference pressure of 5×10^{-4} μb.

[11] The decrease of thermospheric temperature has been inferred from trends of thermospheric neutral density estimated from long-term satellite drag data [e.g., *Keating et al.*, 2000; *Emmert et al.*, 2004, 2008; *Marcos et al.*, 2005]. The estimated density trend at 400 km ranges from −1.7%/decade to −3.0%/decade, for the past 3 to 4 decades. The density trend anticorrelates with solar activity, with trends being approximately −1%/decade to −2%/decade under solar maximum conditions and about −3%/decade to −5%/decade for solar minimum conditions. As expected for a temperature decrease, the density trend increases with altitude. The solar cycle dependence is due to the relative importance of CO_2 infrared cooling and NO infrared cooling. NO density at solar maximum is about three times of that at solar minimum. Consequently, CO_2 cooling is relatively less important at solar maximum. TIMED/SABER measurements revealed a decrease of the global NO cooling rate from 2002 to 2009 by nearly an order of magnitude, while the global CO_2 cooling rate decreased only by 35% [*Mlynczak et al.*, 2010]. These observational findings are qualitatively consistent with modeling results by *Roble and Dickinson* [1989]. Using CO_2 concentrations measured at Mauna Loa, *Qian et al.* [2006] calculated neutral density trend for the period from 1970 to 2000, and found an average density trend of −1.7%/decade at 400 km. Model simulations also showed that this density trend corresponds to a neutral temperature trend of −5.4 K/decade at 400 km. This simulated density trend is in qualitative agreement with the density trends detected from satellite drag data, but at the low end of the range, and lower than the most recent results [*Emmert et al.*, 2008].

[12] Cooling and contraction of the upper atmosphere will likely cause long-term trends in the ionosphere. Trends in the lower ionosphere are relatively well understood [*Laštovička and Bremer*, 2004]. *Bremer* [2008] investigated global trends in the maximum density of the *E* region (N_mE), as represented by its critical frequency (f_oE), based on 71 individual ionosonde stations worldwide. Positive trends dominate but some stations showed negative trends. The average trend in f_oE

was +0.013 ± 0.005 MHz/decade. Trends slightly weaken with increasing latitude; their longitudinal dependence seems to be affected, if not determined, by the longitudinal dependence of ozone trends. *Bremer* [2008] also studied trends in h_mE, the height of the E region peak density. The global trend is −0.29 ± 0.20 km/decade, as an expected consequence of mesospheric cooling and contraction, though there is quite large scatter of trends obtained from data of individual stations. *Bremer* [2008] also analyzed the critical frequency of the F_1 region (f_oF_1) in the same way as f_oE and obtained a weak global positive trend, which is slightly stronger than that for f_oE, with a value of 0.019 ± 0.011 MHz/yr. However, no influence of ozone depletion on trends in f_oF_1 was found, contrary to that in f_oE trends.

[13] Modeling studies on trends in the E and F_1 regions focused on greenhouse gas effects. *Qian et al.* [2008] investigated global mean ionospheric trends due to doubling of CO_2 and their underlying physical mechanisms; in the E and F_1 regions, cooling and contraction decrease the altitude of E and F_1 layers, and increase electron density in these regions. This work was extended to 3D model simulation by *Qian et al.* [2009]. They found that in the E and F_1 regions up to near the F_2 peak, trends of electron density are positive at most of latitudes, above which electron density decreases. These modeling results are consistent with the observational results, at least qualitatively. In addition, trends of electron density in the E region show negative change in a small area near winter high-latitude region whereas trends of electron density in the F_1 region show weak negative change in the equatorial region. It is not clear whether these negative trends can explain the negative E region electron density trends at some stations found by *Bremer* [2008]. Further modeling investigations and model-data comparisons on variability of trends in the E and F_1 regions are needed. These modeling investigations should also consider other possible drivers such as O_3 forcing, trends in natural variability of solar irradiance and geomagnetic activity, and trends of the Earth's magnetic fields.

[14] All the above parameters form a scenario of trends in the upper atmosphere that is consistent with the hypothesis of cooling and contraction of the upper atmosphere due to greenhouse gas forcing. Figure 1 does not show trends for the F_2 region since there have been controversies and discrepancies in data detection of trends. Recent model simulations [*Cnossen and Richmond*, 2008; *Qian et al.*, 2009] demonstrated regional variations and different signs and magnitudes of these trends due to greenhouse gas forcing and evolution of the Earth's magnetic field, which may be able to explain some of the controversies and discrepancies.

3. Trends in the F_2 Region Ionosphere

[15] Trends of F_2 peak density (N_mF_2), its height (h_mF_2), and critical frequency (f_oF_2) have been investigated extensively using the global network of ionosondes. However, controversies and discrepancies remain regarding methods of data analysis, magnitudes of the trends, and interpretation of the causes of the trends. *Laštovička et al.* [2006b] compared results using various methods on a same data set. The calculated trends of f_oF_2 from these methods were predominantly a weak negative trend in the order of −0.1 MHz/decade. *Laštovička et al.* [2008b] found that most trends using various regression-based methods, and a neural network based method [*Yue et al.*, 2006], agreed fairly well with each other; A wavelet-based method was found to be unreliable; only a specific method of Mikhailov [*Mikhailov et al.*, 2002] yielded, after removing the geomagnetic activity effect, a trend of CO_2 origin smaller by more than an order of magnitude and statistically insignificant. There have been two interpretations of the causes of these trends: geomagnetic control and greenhouse gas cooling effects. *Mikhailov and Marin* [2001] introduced the concept of geomagnetic control of trends of f_oF_2 and h_mF_2. *Mikhailov* [2006] further argued that f_oF_2 trends are completely controlled by the long-term variation of geomagnetic activity due to weak dependence of N_mF_2 on neutral temperature. On the other hand, *Danilov* [2002] developed a method of determining long-term trends of nongeomagnetic origin, and found a negative trend in f_oF_2 that supports its anthropogenic origin. Attempts were also made to reconcile the greenhouse and geomagnetic activity causes of these trends. It was suggested that there is simultaneous greenhouse gas control of the trend in h_mF_2, and geomagnetic control of the trend in f_oF_2 [*Mikhailov*, 2006]. However, *Bremer et al.* [2009a] showed that the geomagnetic control dominated in the past but it is no longer the case at present.

[16] Trends of the F_2 peak parameters also exhibit variations with geographic location, local time, season, and solar activity. Controversies exist regarding this variability, and dynamical influence has been used to explain it. *Bremer* [1998] obtained h_mF_2 and f_oF_2 trends of different signs for 31 European stations, with negative trends west of 30°E but positive trends east of 30°E. He suggested that dynamical effects seem to play an important role. On the other hand, *Danilov and Mikhailov* [1999] found negative trends of f_oF_2 for all individual stations they selected, and detected a strong and well pronounced dependence of the f_oF_2 trends on geomagnetic latitude but no longitudinal dependence; this is contrary to Bremer's finding. *Bencze* [2009] found that negative trends in h_mF_2 were observed for stations nearby seashore whereas positive trends were more often found for well-inland stations, and that this distribution of trends may be due to effect of nonmigrating tides. *Danilov* [2008] found long-term variations in the relation between daytime and nighttime f_oF_2 and suggested that long-term variations of thermospheric meridional wind caused these variations. These observed variations in trends of the F_2 peak parameters have also been used as evidence for the origin of these trends. *Mikhailov and Marin* [2000, 2001] suggested that trends of f_oF_2 due to greenhouse gas cooling should be positive and should not have complex latitudinal, longitudinal, and diurnal variations; the observed variability of f_oF_2 trends are evidence of geomagnetic control of the f_oF_2 trend.

[17] Modeling efforts have been made to investigate effect of CO_2 cooling on trends in the ionosphere and the underlying physical mechanisms. *Qian et al.* [2008] showed that on a globally average basis, the response of electron density to increased cooling is positive in the lower ionosphere, but changes to negative in the upper ionosphere. This transition altitude occurs slightly below the F_2 peak. *Qian et al.* [2009] further conducted 3D model simulations of increased greenhouse gases on trends of F_2 peak parameters. The model simulations revealed that the increased greenhouse gases not only caused cooling and contraction of the upper atmo-

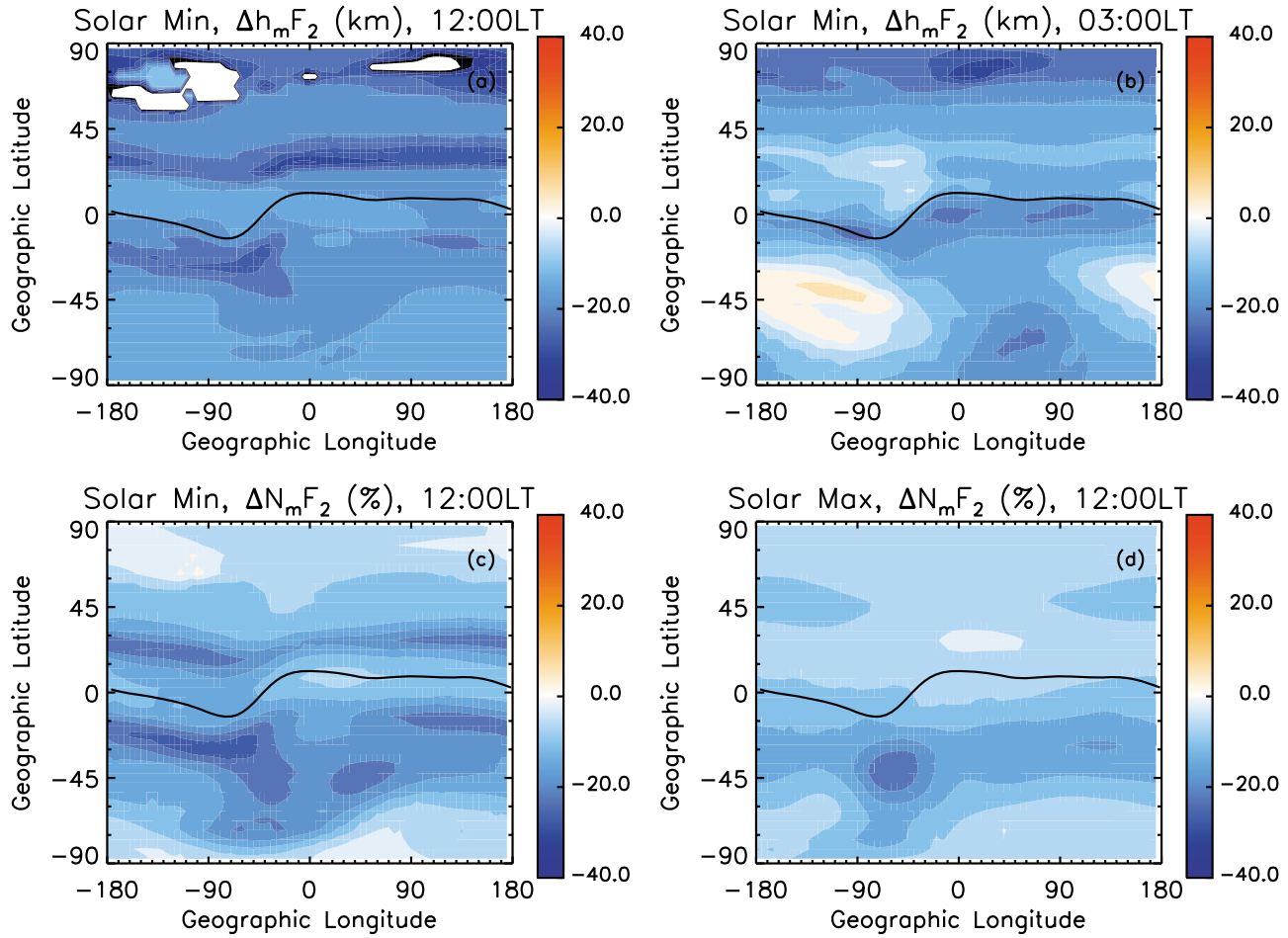

Figure 3. Changes of h_mF_2 and N_mF_2 (double CO_2–base CO_2) under geomagnetic quiet condition, June solstice, simulated by the NCAR TIE-GCM. Changes of h_mF_2 are absolute changes in kilometers, while changes of N_mF_2 are percentage changes. (a) Change of h_mF_2 at local noon, under solar minimum condition; (b) changes of h_mF_2 at 0300 LT, under solar minimum condition; (c) change of N_mF_2 at local noon, under solar minimum condition; and (d) change of N_mF_2 at local noon, under solar maximum condition. Adapted from *Qian et al.* [2009].

sphere, but also changed composition, dynamics, and electrodynamics in the thermosphere and ionosphere. The net effect of these changes determines altitude distributions of trends in the ionosphere, and complex variability of trends of the F_2 peak parameters. Cooling and contraction caused lowering of the E and F_1 layers; in the F_2 region, however, the dynamical effects as well as contraction and composition changes determined trends in the F_2 region. These 3D modeling results are summarized in Figures 3 and 4.

[18] Figure 3 shows the change of h_mF_2 due to doubling of CO_2 at local noon (Figure 3a) and 0300 LT (Figure 3b), under solar minimum and geomagnetic quiet conditions, simulated by the NCAR thermosphere-ionosphere-electrodynamics general circulation model (TIE-GCM) [*Richmond et al.*, 1992]. Trends of h_mF_2 exhibit strong latitudinal, longitudinal, and diurnal variations; they are mostly negative but can be positive at night. *Rishbeth* [1998] found that F_2 peak tends to remain on a same pressure surface as temperature changes. Therefore, the negative change of h_mF_2 is due to cooling and contraction of the upper atmosphere. The positive change of h_mF_2 is due to changes in dynamics as a result of this cooling, as shown in Figure 4.

[19] Figures 3c and 3d show changes of N_mF_2 due to doubling of CO_2 at local noon, for solar minimum and solar maximum, under geomagnetic quiet conditions. On a global average basis, trends of N_mF_2 are larger under solar minimum conditions, and the global distribution of the trends tends to be more structured. Trends of N_mF_2 also show different patterns in the winter and summer hemispheres. Overall, trends of N_mF_2 are larger in the winter hemisphere than in the summer hemisphere, for both solar minimum and maximum conditions.

[20] Figure 4 shows changes of h_mF_2 (Figure 4a) and meridional winds (Figure 4b) due to doubling of CO_2, at 1200 UT, under solar minimum and geomagnetic quiet conditions. There are positive changes of h_mF_2 at nighttime, for example, in the longitude sector between −180° and −90°, where the local time is from 0000 to 0600 LT. Trends of meridional wind are equatorward in both hemispheres. This equatorward trend of the meridional wind has the effect

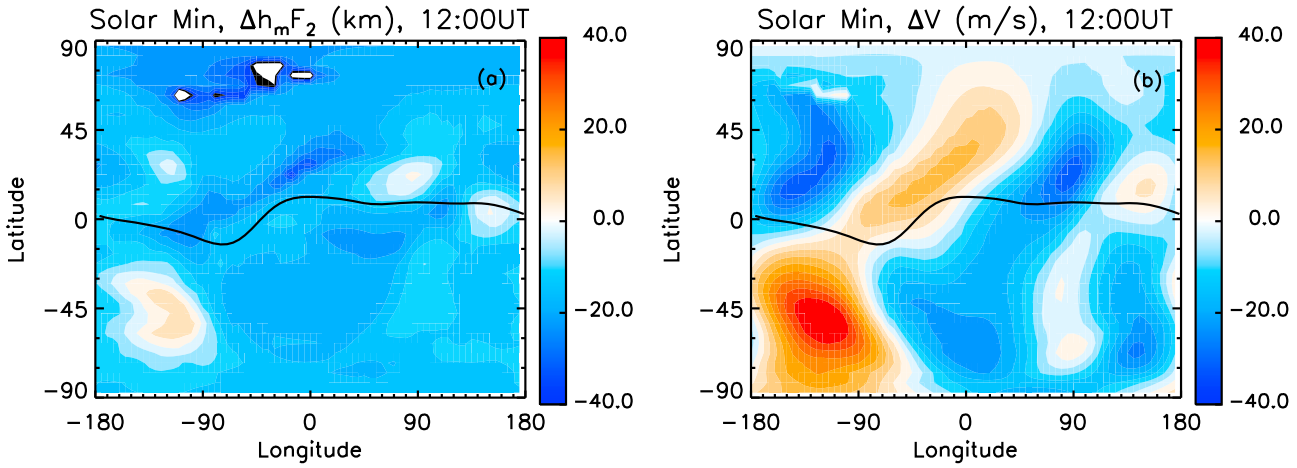

Figure 4. Changes (double CO_2–base CO_2) of (a) h_mF_2 and (b) meridional wind, under solar minimum and geomagnetic quiet conditions, June solstice, at 1200 UT, simulated by the NCAR TIE-GCM. Adapted from *Qian et al.* [2009].

of lifting the F_2 peak to higher pressure surfaces, which compensates the lowering of h_mF_2 due to cooling and contraction. The net effect is a positive change of h_mF_2 in this region.

[21] The effect of long-term change of the Earth's magnetic field on trends of F_2 peak has been examined recently, through modeling investigations [*Cnossen and Richmond*, 2008; *Yue et al.*, 2008] and theoretical analysis [*Elias*, 2009]. Model simulations and theoretical analysis indicated that secular change of the Earth's magnetic field has caused regional trends of h_mF_2 and f_oF_2, and trends of f_oF_2 and h_mF_2 show seasonal and diurnal variations. For example, *Cnossen and Richmond* [2008] examined the effects of secular change of the Earth's magnetic field from 1957 to 1997 on trends of the F_2 peak parameters, using the NCAR TIE-GCM. They found that secular change of the Earth's magnetic field caused changes of h_mF_2 up to ±20 km, and changes of f_oF_2 up to ±0.5 MHz over the low-latitude Atlantic Ocean and South America, but the effect is negligible for the rest of the globe. They also found that secular change of the Earth's magnetic field can explain some of the observed regional variation but not the diurnal and seasonal variation.

[22] There has not yet been a modeling investigation conducted on the effects of long-term changes in geomagnetic activity. Modeling efforts are needed to examine the effect of secular change of geomagnetic activity, as well as to combine the three forcing mechanisms (secular changes of greenhouse gases, the Earth's magnetic field, and geomagnetic activity). It remains to be seen whether modeling results, with all the three forcing mechanisms included, can explain observed regional variation of trends of the F_2 peak parameters; and their diurnal, seasonal, and solar cycle variability.

[23] We have so far discussed trends of h_mF_2 and f_oF_2. Recently, progress has been made on trends of ion temperature in the F_2 region. *Holt and Zhang* [2008] investigated trends of ion temperature using long-term ion temperature data measured by incoherent scatter radar (ISR) above Millstone Hill. They found a negative trend of ion temperature of −47 K/decade at 375 km, for the period from 1978 to 2007. Figure 5 shows TIME-GCM simulated changes of

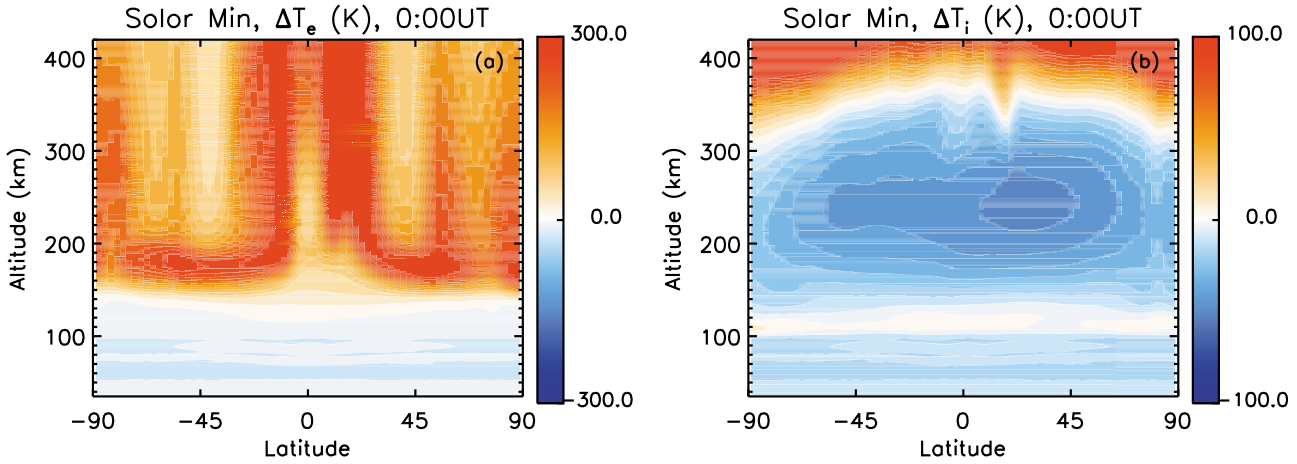

Figure 5. Changes (double CO_2–base CO_2) of (a) zonal mean electron temperature and (b) zonal mean ion temperature, under solar minimum and geomagnetic quiet conditions, at 0000 UT, simulated by the NCAR TIME-GCM.

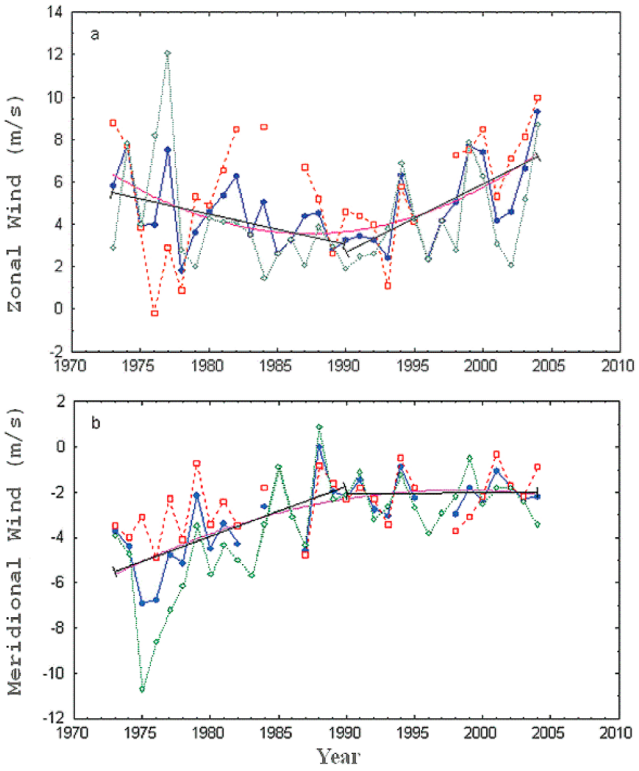

Figure 6. MLT annual mean prevailing winds over Obninsk (55°N, 37°E) and Collm (52°N, 15°E): red, Obninsk; green, Collm; blue, mean values. (a) Zonal component and (b) meridional component. From *Laštovička et al.* [2008a].

zonal mean electron and ion temperature due to doubling of CO_2 at 0000 UT, under solar minimum and geomagnetic quiet conditions. There is a positive change of electron temperature caused by the negative trend of electron density in the upper F_2 region. The model simulations were based on the assumption that the energy input from the magnetosphere to the thermosphere/ionosphere system through plasma transport was same, for the base case and the doubling case. Under this assumption, the negative change of electron density causes a positive change in electron temperature, as shown in Figure 5a. A positive trend of electron temperature was also found in the long-term ISR data over Millstone Hill used (S. Zhang, private communication, 2010).

[24] Figure 5b shows the corresponding change of ion temperature. The change of ion temperature is negative below the altitude ~350 km, on the order of −50 K. This indicates coupling between ion and neutral temperature as cooling in the thermosphere causes cooling in ion temperature in this altitude region. Above ~350 km, the change of ion temperature becomes positive. This indicates coupling between ion and electron temperature since the change of electron temperature is positive. There are two discrepancies between the data results and the modeling results. The magnitude of the negative change of ion temperature from *Holt and Zhang* [2008] (−47 K/decade) is much larger that that from the model simulation (~−50 K for doubling of CO_2), considering that the change of CO_2 concentration during the three decades from 1978 to 2007 is only about 12%. Also, the positive change of ion temperature at lower altitude is not seen in the data. *Zhang and Holt* [2011] found only small and statistically insignificant trends in ion temperature below about 250 km. The negative trends peaked at 350–400 km but were still negative, strong and significant in the exospheric ion temperature. Further modeling and data analysis are needed to understand these discrepancies.

[25] Similar to the F_2 region trends, another two areas that have had controversies or limited knowledge, but where recent progress has occurred, are trends in the MLT dynamics and trends in water vapor related phenomena. These two areas will be discussed in sections 4 and 5.

4. Trends in MLT Dynamics and Waves

[26] Routine wind measurements in the MLT region (80–100 km) have been made for several decades. Long-term trends of prevailing wind and semidiurnal tides have been examined and detected using long-term wind measurements at midlatitude to high-latitude stations in the northern hemisphere [e.g., *Portnyagin et al.*, 2006]. Figure 6 shows time series of annual mean zonal and meridional prevailing winds over Obninsk (55°N, 37°E) and Collm (52°N, 15°E). In spite of differences in the measurement techniques and strong year-to-year wind variations, the general tendencies in the climatic MLT wind variations at both stations are similar. Before 1990, both the annual prevailing zonal and meridional wind weakened, while after 1990, zonal wind strengthened and the negative trend in meridional wind leveled off. Shorter-period wind data series from some other stations confirmed that this change of trend is characteristic for the Northern Hemisphere midlatitude belt.

[27] Amplitudes of diurnal and semidiurnal tidal components has weakened, but various data indicate that the negative trend ceased after the mid 1980s or near 1990 [*Jacobi et al.*, 1997; *Portnyagin et al.*, 2006], or even reversed. The most recent results from Collm, however, indicate negative trend (weakening) of the semidiurnal tide (with large seasonal variation of trend) over 1979–2007. More observations are needed.

[28] The change of trends around 1990 occurs not only in the MLT prevailing wind, it also occurs in the lower stratospheric winds at 100 hPa at 50–70°N, in the occurrence frequency of small laminae in ozone profiles in Europe near 50°N [*Laštovička et al.*, 2010], and in the stationary planetary wave with zonal wave number one near 50°N [*Jacobi et al.*, 2009]. This indicates the possibility of changes in trends in dynamics of the entire northern midlatitude middle atmosphere. One of the principal sources of small laminae in ozone profiles is upward propagating gravity wave. This suggests that the change of trends in various parameters around 1990 may be caused by a change in trend in gravity wave activity, at least, partly.

[29] Waves play an important role in dynamics and energy deposition in the MLT region. Sources and atmospheric filtering of these waves might be affected by anthropogenic changes in the atmosphere. MLT dynamics is forced through wave coupling, so trends in the mean circulation may be indicative of possible long-term trends in wave activity. The MLT wave activity is mainly from waves that are generated in the troposphere and some in the stratosphere, and propagate upward into this region. Therefore, their trends might

differ from trends of in situ mesospheric parameters. The wave propagation conditions in the stratosphere/mesosphere and various interaction processes in the MLT region contribute substantially to resulting MLT wave activity. Usually, wave activity is divided into three main categories: gravity waves with periods of tens of minutes to hours, tides with periods of 24 h and harmonics, and planetary waves with periods of about 2–30 days.

[30] Information on trends in planetary wave activity as summarized by *Laštovička et al.* [2008a] does not provide a clear pattern. Planetary wave activity in the MLT region appears to have increased, even though this increase seems to be intermittent. *Jacobi et al.* [2008] reported trends in planetary wave activity, which were highly variable with period range and season, being generally positive in zonal wind and weaker and negative in meridional wind, and in total wind being slightly positive on average. They observed some trends only for quasi 5 day waves and the overall (2–30 days) wave activity; whereas for other period ranges, the trends were weak if any. The obtained trends were statistically insignificant except for peak trends in summer for the quasi 5 day (3–7 days) oscillations.

[31] Results of gravity wave analyses from ground-based systems can be strongly dependent on system characteristics. The wave periods seen in wind data measured by MF radars (>10 min), meteor radars (>1h), and LF drifts (0.7–3h) are very different and results are not comparable. There are some indirect indications of possible trends in gravity wave activity in the MLT region [e.g., *Jacobi et al.*, 2006] but direct wind measurements did not reveal a trend [*Gavrilov et al.*, 2002]. *Hoffmann et al.* [2010] found for Juliusruh (northern Germany) a weak positive trend at 80–90 km and they mentioned that some stations displayed trends, others not. Information on trends in the MLT region gravity wave activity is still very limited. Potential mechanisms of trends in gravity wave activity may be related either to changes in middle atmosphere filtering, or to changes in tropospheric/stratospheric sources such as deep tropical convection or changes of storm tracks at midlatitudes; the latter may result in regionally/locally different trends in gravity wave activity even as to sign of trends.

[32] Systematic modeling studies regarding long-term trends of the MLT dynamics and waves have not previously been conducted. Here, we show preliminary results from TIME-GCM simulations of changes of MLT neutral winds due to doubling of CO_2. Figure 7 shows zonal wind for the base case (Figure 7a), the doubling case (Figure 7b), and the difference of the two cases (Figure 7c), at 0000 UT and 41.25°N, under solar minimum and geomagnetic quiet conditions. The patterns of semidiurnal tides in the MLT region are similar for the base case and the doubling case, but amplitudes of the semidiurnal tides are different. Change of the zonal wind speed is in the order of 10 m/s (Figure 7c). This is a significant change considering that the zonal wind in this altitude region is in the order of 50 m/s. These results indicate that MLT dynamics will have a long-term trend under greenhouse gas forcing. However, more elaborated model simulations are needed for model-data comparison. For example, trends in O_3 and H_2O concentrations have significant influence on trends of temperature and neutral density in the MLT region [*Akmaev et al.*, 2006], which will likely affect trends of MLT dynamics.

[33] There is no direct observational information about trends in winds in the thermosphere. However, *Danilov* [2009a, 2009b] and *Danilov and Vanina-Dart* [2010] used the behavior of ionospheric parameters f_oF_2 and h_mF_2, including their scatter, to deduce changes of trends in thermospheric dynamics. They found no trend before about 1980 but a systematic long-term trend after about 1980, which they attributed to cooling of the middle and upper atmosphere.

5. Trends in Water Vapor–Related Phenomena

[34] According to regular frost point hygrometer balloon-borne measurements, water vapor content in the lower stratosphere has increased by ~1%/yr over the last 40–45 years of the 20th century [*Oltmans et al.*, 2000]. An updated trend analysis of water vapor in the lower midlatitude stratosphere from the Boulder balloon-borne frost point hygrometer measurements and from HALOE [*Scherer et al.*, 2008] resulted in two corrections for instrumental bias. The new linear trend for the period 1980–2000 is estimated at 0.6 to 0.7%/yr. In addition, HALOE, POAM, and balloon measurements have shown a considerable decrease in lower stratospheric water vapor, by ~0.4 ppmv, following a sudden drop in 2001, which appears to coincide with anomalous cooling of the tropical tropopause [*Randel et al.*, 2006]. MIPAS stratospheric water vapor measurements [*Stiller et al.*, 2008] revealed, following the drop in 2001, a continuous increase of stratospheric water vapor since 2002. However, another decrease appeared in 2008–2009, and at present the water vapor concentration in the stratosphere is below the 2000 level [*Solomon et al.*, 2010a]. The water vapor puzzle remains to be solved. Similar to trends in dynamics, trends in water vapor are largely determined by trends in tropospheric sources and conditions of upward propagation and, therefore, can hardly be directly comparable with other trends in the mesosphere region.

[35] The highest atmospheric clouds observed from the ground, noctilucent clouds (NLC), appear in the extremely cold summer polar mesopause region at heights of about 82 to 85 km. The same phenomenon, observed from above by satellites, is called polar mesospheric clouds (PMC). Their appearance is controlled by temperature and water vapor content. Long-term trends in the occurrence frequency and brightness of NLCs observed from the ground, at latitudes below about 65°N in Europe, do not display a detectable trend in the NLCs, according to *Kirkwood et al.* [2008]. Satellite observations cover a larger geographical area and the highest occurrence frequency of PMCs is around 80°N. The satellite observations indicate an increase in PMC occurrence frequency and brightness. *Shettle et al.* [2009] analyzed 28 years of satellite PMC observations for latitudinal bands 50°N–64°N (NLC observation latitudes), 64°N–74°N, and 74°N–82°N. They observed a statistically significant increase only at 74°N–82°N, whereas at 50°N–64°N, the increase was half the magnitude and statistically insignificant. At NLC observational latitudes, the PMC trend of *Shettle et al.* [2009] is +9.9%/decade, the NLC trend of *Kirkwood et al.* [2008] is +4.4%/decade for moderate and bright NLCs, and ~14%/decade for all NLCs; all trends being statistically insignificant. This means that the PMC and NLC trends are comparable, and do not differ within

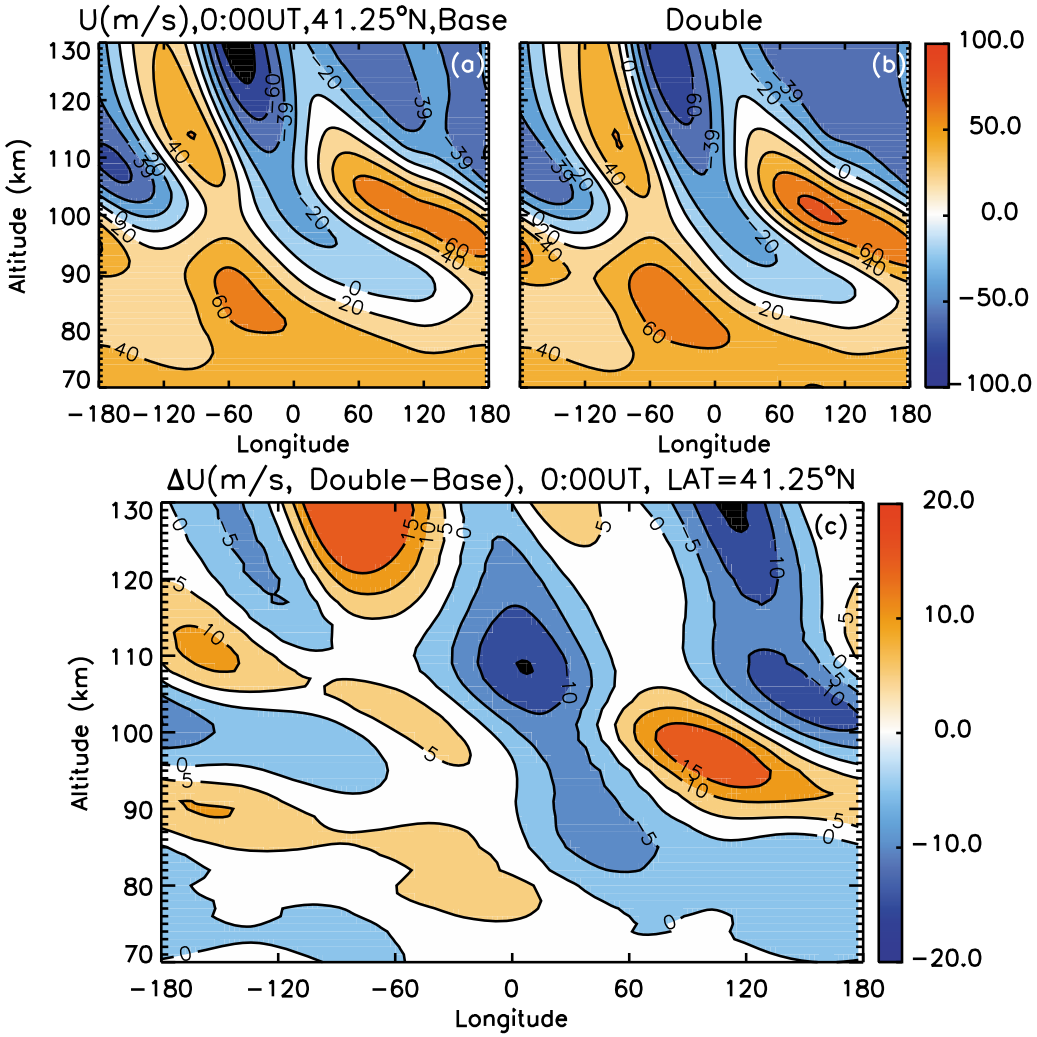

Figure 7. Zonal wind and change (double CO_2–base CO_2) of the zonal wind at 41.25°N, under solar minimum and geomagnetic quiet conditions, at 0000 UT, simulated by the NCAR TIME-GCM. (a) Zonal wind for the base case, (b) zonal wind for the doubling case, and (c) change of the zonal wind between the two cases.

accuracy of their determination, in spite of differences in the analysis intervals.

[36] Polar mesospheric summer echoes (PMSE), the anomalous radar echoes found between 80 and 90 km from May through early August in the Arctic, and from November to February in the Antarctic, are phenomena closely related to PMC. *Bremer et al.* [2009b] found a positive but insignificant trend in PMSE occurrence frequency and length of season for Andenes (69°N) over 1994–2008, whereas *Smirnova et al.* [2010] found insignificant negative and positive trends, for Kiruna (68°N) over 1997–2008.

[37] Simulations with the LIMA/ice model [*Lübken et al.*, 2009] show that all three factors, temperature, water vapor, and Lyman-α solar radiation, are important and none of them is dominant in PMC/NLC behavior. There is no detectable temperature trend in the mesopause NLC/PMC heights. Water vapor trends in the mesopause region are uncertain. However, *Lübken et al.* [2010] found that the occurrence frequency of NLC is determined mainly by water vapor concentration, whereas the NLC height is affected predominantly by temperature. Further investigations are necessary on possible trends of NLC/PMC and origin of the trends.

6. Drivers of Trends

[38] Based on observational and modeling studies, the dominant driver for trends in the upper atmosphere and ionosphere has been attributed to the increasing greenhouse gas forcing, mainly CO_2; other drivers are secular changes of geomagnetic activity, the Earth's magnetic field, other radiatively active trace gases such as O_3, H_2O, and CH_4. In addition, atmospheric waves may also have had secular change in the past several decades, and this possible secular change may have played a role in long-term trends of the upper atmosphere and ionosphere; however, this remains to be speculative.

[39] Figure 8 shows changes of neutral temperature, CO_2 15 μm cooling, NO 5.3 μm cooling, and total radiative cooling due to doubling of CO_2, under solar minimum and

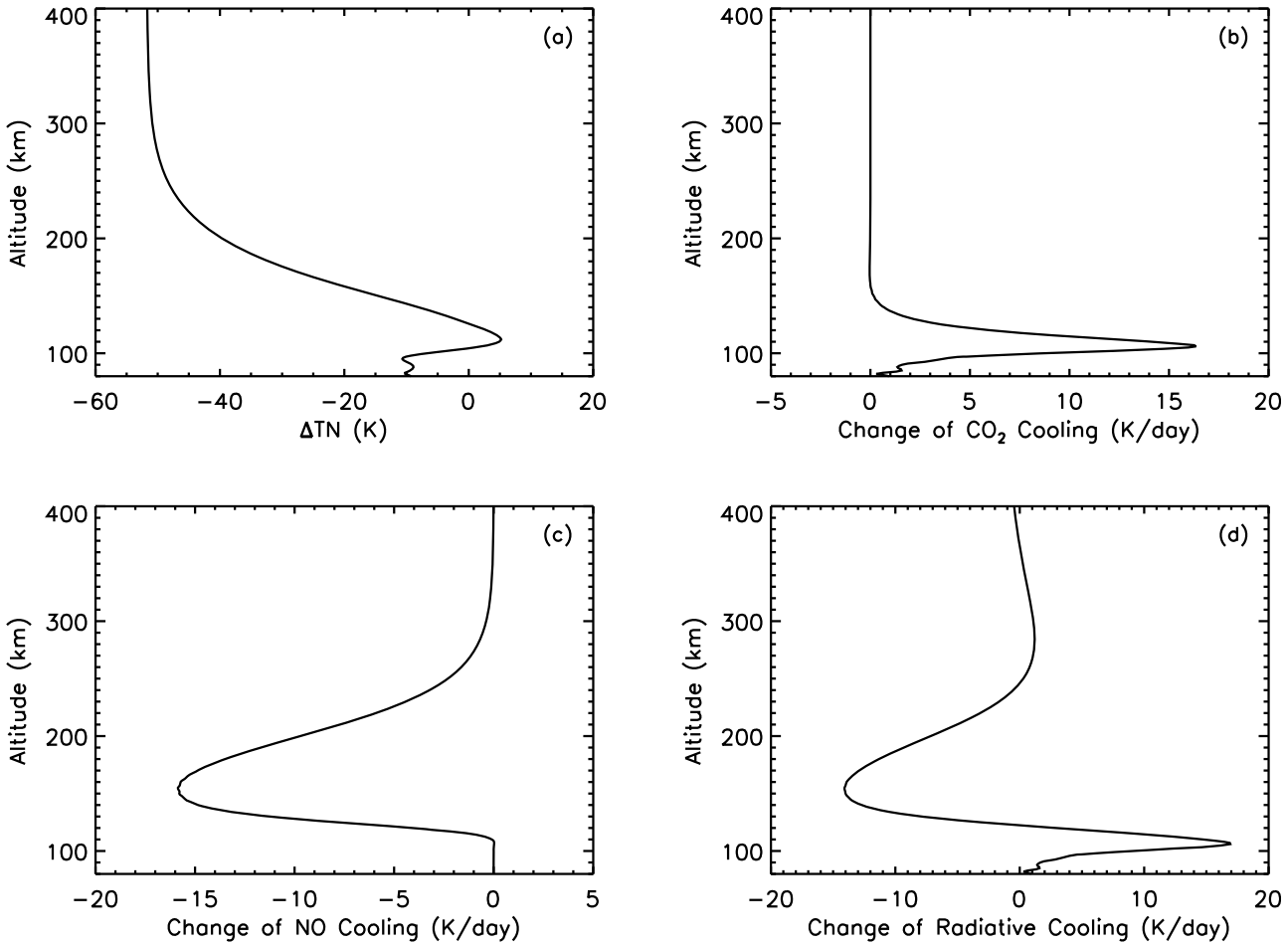

Figure 8. Global mean changes (double CO_2–base CO_2) of (a) neutral temperature, (b) CO_2 15 μm cooling, (c) NO 5.3 μm cooling, and (d) total radiative cooling at 0000 UT, under solar minimum and geomagnetic quiet conditions, simulated by the NCAR TIME-GCM.

geomagnetic quiet conditions, simulated by the TIME-GCM. CO_2 cooling increases due to the increased CO_2 concentration (Figure 8b). However, NO cooling decreases responding to the increased CO_2 cooling (Figure 8c). The decrease of NO cooling is due to decrease in NO and O concentration at fixed altitude, as well as decrease in temperature (Figure 8a). The decrease of NO cooling reduces the total radiative cooling (Figure 8d). Therefore, NO cooling modulates the cooling and contraction of the upper atmosphere due to the CO_2 forcing. Model simulation indicated that thermospheric cooling due to CO_2 forcing would be twice as large without this modulation.

[40] Cooling and contraction of the upper atmosphere change neutral and ion composition. The ionosphere in the E and F_1 regions is approximately in photochemical equilibrium. Therefore, electron density in the E and F_1 regions is determined by neutral and ion composition, solar irradiance, and temperature. Thermospheric cooling has the effect of increasing the ionization rate due to reduced absorption above these regions, increasing the ratio of O to N_2, and reducing the ratio of NO^+ and O_2^+, the major ions in the E region [*Qian et al.*, 2008]. The net effect is an increase of electron density in the E and F_1 regions. In the F_2 region, plasma transport becomes increasingly important. The combined effect of changes in photochemical and plasma transport processes is a slight decrease of electron density at F_2 peak and a large decrease of electron density above the F_2 peak. In addition, the interplay of photochemical and plasma transport processes causes complex regional, diurnal, seasonal, and solar cycle variations of trends in the ionosphere [*Qian et al.*, 2009].

[41] *Mikhailov and Marin* [2001] proposed secular change of geomagnetic activity as the mechanism for trends of f_oF_2 and h_mF_2. They suggested that periods with negative and positive f_oF_2 and h_mF_2 trends correspond to periods of increasing or decreasing geomagnetic activity, as a consequence of changes of neutral composition, temperature, and neutral wind due to change of geomagnetic activity. Geomagnetic activity increased during the course of the 20th century [*Clilverd et al.*, 1998; *Mursula and Martini*, 2006], and solar activity was increasing till 1957–58. The increase of geomagnetic activity leveled off and might even be decreasing at present. *Laštovička* [2005] examined the role of solar and geomagnetic activity in trends in the upper atmosphere and ionosphere, concluding that the role of solar and geomagnetic activity in the observed long-term trends decreases with decreasing altitude; in the 20th century, the role of solar and geomagnetic activity in the observed

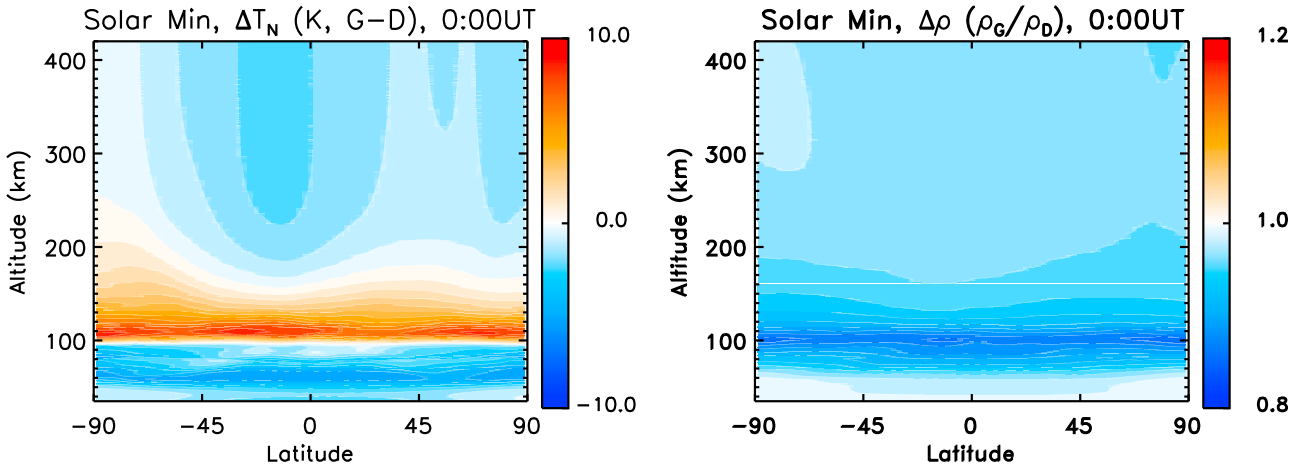

Figure 9. Changes of zonal mean neutral temperature and neutral density due to trace gases other than CO_2, such as O_3 depletion (halved), H_2O increase (doubled), and CH_4 increase (doubled) (see Table 1), under solar minimum and geomagnetic quiet conditions, at 0000 UT, simulated by the NCAR TIME-GCM: D, the simulation case with doubling of CO_2 only; G, the simulation case with doubling of CO_2 plus changes of concentrations of all the other gases shown in Table 1.

long-term trends was decreasing from its beginning toward its end. *Bremer et al.* [2009a] found that the change of dependency of trends on secular change of geomagnetic activity occurred around 1970 in the *E* region, confirming earlier findings by *Mikhailov and de la Morena* [2003], in the mid-1990s in the F_1 region, and around 2000 in the F_2 region. As for the effect of secular change in solar activity, it is clear that any secular variation in solar ultraviolet irradiance will cause secular trends in temperature and neutral density in the upper atmosphere, which in turn will cause trends in the ionosphere. Estimation of thermospheric trends in the presence of large solar-driven variation is a particular challenge in the highly variable upper thermosphere, especially since recent observations show that the solar minimum period during 2008–2009 was anomalously low in density compared to previous minima, even after the effects of anthropogenic trends are accounted for [*Emmert et al.*, 2010]. This may have been due in part to lower levels of solar EUV irradiance [*Solomon et al.*, 2010b].

[42] The impact of long-term changes of the Earth's magnetic field has been examined through model simulations [*Cnossen and Richmond*, 2008; *Yue et al.*, 2008] and theoretical analysis [*Elias*, 2009]. It is found that secular change of magnetic field caused significant trends of f_oF_2 and h_mF_2 in the equatorial to midlatitude Atlantic Ocean and in the South American but its effect is negligible in the rest of globe. *Cnossen and Richmond* [2008] found that most of the modeled changes in h_mF_2 and f_oF_2 were due to plasma transport driven by neutral winds, which are mainly caused by changes in the inclination of the magnetic field, with a secondary role due to changes in declination.

[43] Similar to CO_2, changes in other radiatively active trace gases can also cause trends in the upper atmosphere. Stratospheric O_3 depletion has been observed since 1979 with a turnaround of the trend at northern middle latitudes near 1995, which appears to be caused primarily by atmospheric dynamics [*Harris et al.*, 2008]. On the other hand, stratospheric water vapor has increased for the last several decades [*Oltmans et al.*, 2000; *Scherer et al.*, 2008; *Stiller et al.*, 2008]. *Akmaev et al.* [2006] simulated trends of temperature and neutral density in the MLT region due to estimated trends of CO_2, O_3, and H_2O, from 1980 to 2000. They found that O_3 depletion caused cooling in the mesosphere due to reduced solar heating, and the O_3 forcing is comparable to the CO_2 forcing. H_2O enhancement also caused cooling in the mesosphere due to increased infrared emission, but the effect of the H_2O forcing is minor compared to the O_3 and CO_2 forcing. In addition, O_3 depletion and H_2O enhancement caused some warming in the lower thermosphere near 120 km, due to contraction of the MLT region and the large positive temperature gradient in the lower thermosphere. Furthermore, O_3 depletion and H_2O increase caused maximum reduction of neutral density near 110 km. Figure 9 shows TIME-GCM simulated changes of temperature and neutral density due to estimated changes of trace gases other than CO_2, as shown in Table 1. Forcing from these trace gases caused additional cooling in the mesosphere, slight cooling in the upper thermosphere, but some warming in the altitude region around 100–120 km (appearing only in height coordinates, not in pressure coordinates); it caused neutral density decrease in the mesosphere and thermosphere with maximum density reduction around 110 km. These results are consistent with the results by *Akmaev et al.* [2006]. Although modeling studies have demonstrated that trends of these trace gases can cause trends in the upper atmosphere, observational studies are still very limited. In the ionosphere, clear anticorrelation between f_oE trend deviations and total ozone trend deviations has been observed [*Bremer and Peters*, 2008]; whereas no relation has been detected between trends in the F_1 region and the O_3 trend [*Bremer*, 2008]. The effect of long-term change of these trace gases can also be detected through other parameters. Calculations of the atomic hydrogen budget, which is a product of CH_4 dissociation, predict a large increase in exospheric H. Long-term geocoronal hydrogen observations [*Nossal et al.*, 2008] are now available to investigate long-term changes in exospheric hydrogen.

Table 1. Minor Species and Their Concentrations (ppmv) Based on Work by *Crutzen and Brühl* [1993] Used in TIME-GCM Simulations

Species	Base Case	Test Case
CH_4	0.6	1.34
H_2	0.5	1.0
CO	1.1E-2	2.2E-2
H_2O	4.4	8.8
NO	2.7E-3	16.0E-3
NO_2	4.2E-3	8.4E-3
O_3	8.3	4.15

[44] The turnaround of stratospheric ozone trends resulted in the leveling off of trends in stratospheric temperatures [*Schwarzkopf and Ramaswamy*, 2008]. HALOE trends in mesospheric temperatures are weaker than older rocket and lidar-based trends, as the net ozone effect over the period of HALOE observations was close to zero [*Remsberg*, 2009]. In the mesopause region the turnaround of ozone trends resulted in a change from no trend to a mild negative trend, at least at low latitudes [e.g., *Venkat Ratnam et al.*, 2010].

[45] Information on trend of waves in the MLT region, as well as its role on trends in the upper atmosphere and ionosphere, remains to be speculative. There are some indications of possible trends in gravity wave activity [e.g., *Jacobi et al.*, 2006], tides [e.g., *Portnyagin et al.*, 2006], and planetary waves [e.g., *Jacobi et al.*, 2008]. Long-term changes in the waves can be caused by their sources in the troposphere and stratosphere, as well as their propagation environment which is the large-scale circulation in the stratosphere and mesosphere. The possible trends in wave activity can then be a driver to long-term change in the upper atmosphere. Trends in some middle and upper atmosphere parameters have shown a turnaround in the 1990s. For example, this turnaround has been shown in trends of NH midlatitude total ozone [*Harris et al.*, 2008], temperature at 83 km, and NLC centroid height [*Lübken et al.*, 2009]. Changes in trend of gravity wave activity could have contributed to this turnaround.

[46] Greenhouse gas concentration is steadily and more or less homogeneously increasing. However, other drivers change with time and sometimes also with location. Geomagnetic activity was increasing throughout the 20th century but leveled off, and solar activity was increasing till 1957–58; Secular changes of the Earth's magnetic field are very regional phenomenon and introduces regional trends; Stratospheric O_3 has decreased since 1979 but with a turnaround of the trend near 1995, its changes are large at high latitudes but almost negligible at low latitudes, and to some extent also longitude dependent; stratospheric water vapor has increased for the last several decades but had a drop in 2001; Possible trends in atmospheric wave activity are probably also unstable. Therefore, we can hardly expect stable, monotonic trends, and constant roles of the various drivers.

7. Conclusions and Future Direction of Investigations

[47] The steady increase of greenhouse gas concentrations, mainly CO_2, has caused global warming in the troposphere, but global cooling in the upper atmosphere and ionosphere. In the mesosphere, the cooling trend is in the order of −2 to −3 K/decade from 50 km to 80 km, but significant cooling has not been clearly identified in the mesopause region from 80 km to 100 km. However, the recent turnaround of ozone trends seems to influence to some extent temperature trends in the stratosphere [*Schwarzkopf and Ramaswamy*, 2008] as well as the mesosphere [e.g., *Remsberg*, 2009; *Venkat Ratnam et al.*, 2010]. In the upper thermosphere, the decreasing trend of neutral density inferred from satellite drag analysis is in the range −1.7 to −3.0%/decade at 400 km, for the past several decades. The cooling and contraction of the upper atmosphere lowers the altitude of ionospheric layers, with a global average trend in the order of -0.29 ± 0.20 km/decade at E region peak. In addition, a long-term global increase of electron density has been detected in these regions, in the order of $+0.013 \pm 0.005$ MHz/decade for f_oE and 0.019 ± 0.011 MHz/yr for f_oF_1. The dominant driver of these trends has been attributed to the increasing greenhouse gas forcing. Various model simulations of long-term trends of the upper atmosphere and ionosphere agree at least qualitatively with these detected trends. Other forcing mechanisms such as changes in other radiatively active trace gases (e.g., O_3 and H_2O), long-term change in geomagnetic activity, and long-term change in the Earth's magnetic field, also contribute to the observed trends. The combined effects and changing roles of the drivers can cause complicated patterns of trends; this is particularly true in the F_2 region.

[48] Trends in the F_2 region ionosphere, MLT dynamics and waves, and water vapor related phenomena, are three areas that have been among the most controversial. Progress has been made in the past few years in these areas. For the F_2 region ionosphere, model simulations demonstrated that under greenhouse gas forcing, the trend of electron density changes from being positive in the E and F_1 regions to negative in the upper F_2 region, with the transitional altitude slightly below the F_2 peak. Consequently, the trend of N_mF_2 is expected to be small and negative on a global average basis, even as h_mF_2 declines due to cooling and contraction. Trends of both h_mF_2 and N_mF_2 show strong latitudinal, longitudinal, diurnal, and solar cycle variability due to changes in neutral dynamics and electrodynamics, which in turn can cause positive trends of h_mF_2 and N_mF_2 at night in some regions. Model simulations also show that secular change of the Earth's magnetic field can cause significant regional trends of h_mF_2 and N_mF_2, especially in the Atlantic sector. The sign of the trends can be positive or negative, depending on region, and these trends also show diurnal and seasonal variations. Furthermore, gradual changes in geomagnetic activity can contribute to ionospheric trends. The combined effects of these drivers and the changing role of geomagnetic activity, as well as difficulty in removing solar cycle influences in trend analysis, have likely contributed to controversies and discrepancies with F_2 region analyses. In addition, a negative trend in ion temperature has been found in ISR data. However, the estimated decrease is much larger than neutral atmosphere changes inferred from satellite drag data, and model simulations have not been able to explain such a large change in ion temperature.

[49] Although it is now generally acknowledged that PMC and NLC are the same phenomenon observed from different locations, discrepancies between observed trends in mesospheric cloud detection have persisted. There has been an increase in PMC (observed from space) occurrence frequency

and brightness in the past several decades, but no detectable trend in NLC (observed from the ground) was seen. More recent studies found that PMC trends are only significant in the latitude band from 74°N to 82°N, but at NLC observational latitudes (~54°N to ~64°N), both PMC and NLC trends are statistically insignificant. These findings may explain and reconcile the discrepancies between PMC and NLC trends.

[50] Limited observational studies indicate possible trends in wave activity. However, knowledge of trends of MLT dynamics is still very limited. Changes in waves and tides, both as consequences of global change in the lower and middle atmosphere, and as a possible driver of trends in the upper atmosphere and ionosphere, is one of the critical open questions regarding trends in the upper atmosphere and ionosphere.

[51] Continued progress in understanding and predicting upper atmosphere global change will entail contributions from ongoing measurements of these changes, monitoring of the anthropogenic and natural drivers, and model development and improvement incorporating the evolving inputs. Analysis of long-term data sets, sometimes derived from changing technology, can be challenging, but it is imperative to continue both the acquisition and interpretation processes. In addition to continuing work on trends from satellite drag and ground-based ionosphere measurements, measurement of middle atmosphere dynamics, temperature, and water vapor, clouds and airglow in the mesopause region, and exospheric hydrogen emissions will be important components. Measurements of critical energy inputs and outputs to the upper atmospheric system, particularly solar ultraviolet irradiance and infrared cooling rates, are also essential. These provide the basic information needed for theoretical and modeling studies to fully quantify the causes and consequences of changes to the upper atmosphere and space environments. Particular challenges for model development include combined simulations of anthropogenic and geomagnetic change, improvement of the treatment of electron and ion temperature calculations, evaluation of collisional excitation rates and other chemical control of cooling rates, and incorporation of accurate solar inputs. The integration of upper atmosphere models with lower atmosphere and Earth system models for comprehensive simulation of the entire terrestrial climate system will be an essential step toward addressing questions on how atmospheric dynamics will respond to global change. Future advances on these problems will depend on maintaining comprehensive international programs supporting atmospheric measurement, trend analysis, and model comparison.

[52] **Acknowledgments.** This work was supported by NASA grants NNX08AQ31G and NNX10AF21G to the National Center for Atmospheric Research and by GACR grant P209/10/1792 to the Institute of Atmospheric Physics of Czech Republic. NCAR is sponsored by the National Science Foundation.

[53] Robert Lysak thanks Gufran Beig and Frank Marcos for their assistance in evaluating this paper.

References

Akmaev, R. A., and V. I. Fomichev (2000), A model estimate of cooling in the mesosphere and lower thermosphere due to the CO_2 increase over the last 3–4 decades, *Geophys. Res. Lett.*, *27*, 2113–2116, doi:10.1029/1999GL011333.

Akmaev, R. A., V. I. Fomichev, and X. Zhu (2006), Impact of middle-atmospheric composition changes on greenhouse cooling in the upper atmosphere, *J. Atmos. Sol. Terr. Phys.*, *68*, 1879–1889, doi:10.1016/j.jastp.2006.03.008.

Beig, G. (2006), Trends in the mesopause region temperature and our understanding—An update, *Phys. Chem. Earth*, *31*, 3–9.

Beig, G., et al. (2003), Review of mesospheric temperature trends, *Rev. Geophys.*, *41*(4), 1015, doi:10.1029/2002RG000121.

Bencze, P. (2009), Geographical distribution of long-term changes in the height of the maximum electron density of the *F* region: A nonmigrating tidal effect?, *J. Geophys. Res.*, *114*, A06304, doi:10.1029/2008JA013492.

Bittner, M., D. Offermann, H.-H. Graef, M. Donner, and K. Hamilton (2002), An 18-year time series of OH rotational temperatures and middle atmosphere decadal variations, *J. Atmos. Sol. Terr. Phys.*, *64*, 1147–1166, doi:10.1016/S1364-6826(02)00065-2.

Bougher, S. W., and R. G. Roble (1991), Comparative terrestrial planet thermospheres: 1. Solar cycle variations of global mean temperatures, *J. Geophys. Res.*, *96*, 11,045–11,055, doi:10.1029/91JA01162.

Bremer, J. (1998), Trends in the ionospheric *E*- and *F* regions over Europe, *Ann. Geophys.*, *16*, 986–996, doi:10.1007/s00585-998-0986-9.

Bremer, J. (2008), Long-term trends in the ionospheric *E* and *F*1 regions, *Ann. Geophys.*, *26*, 1189–1197, doi:10.5194/angeo-26-1189-2008.

Bremer, J., and D. Peters (2008), Influence of stratospheric ozone changes on long-term trends in the meso- and lower thermosphere, *J. Atmos. Sol. Terr. Phys.*, *70*, 1473–1481, doi:10.1016/j.jastp.2008.03.024.

Bremer, J., et al. (2009a), Climate of the upper atmosphere, *Ann. Geophys.*, *52*, 273–299.

Bremer, J., P. Hoffmann, R. Latteck, W. Singer, and M. Zecha (2009b), Long-term changes of (polar) mesosphere summer echoes, *J. Atmos. Sol. Terr. Phys.*, *71*, 1571–1576, doi:10.1016/j.jastp.2009.03.010.

Cicerone, R. J. (1990), Greenhouse cooling up high, *Nature*, *344*, 104–105, doi:10.1038/344104a0.

Clemesha, B. R., D. M. Simonich, and P. P. Batista (1992), A longterm trend in the height of the atmospheric sodium layer: Possible evidence for global change, *Geophys. Res. Lett.*, *19*, 457–460, doi:10.1029/92GL00123.

Clilverd, M. A., T. G. C. Clark, E. Clarke, and H. Rishbeth (1998), Increased magnetic storm activity from 1868 to 1995, *J. Atmos. Sol. Terr. Phys.*, *60*, 1047–1056, doi:10.1016/S1364-6826(98)00049-2.

Cnossen, I., and A. D. Richmond (2008), Modelling the effect of changes in the Earth's magnetic field from 1957 to 1997 on the ionospheric *hmF*2 and *foF*2 parameters, *J. Atmos. Sol. Terr. Phys.*, *70*, 1512–1524, doi:10.1016/j.jastp.2008.05.003.

Crutzen, P. J., and C. Brühl (1993), A model study of atmospheric temperatures and the concentrations of ozone, hydroxyl, and some other photochemically active gases during the glacial, the preindustrial Holocene and the present, *Geophys. Res. Lett.*, *20*, 1047–1050, doi:10.1029/93GL01423.

Danilov, A. D. (2002), The method of determination of long-term trends in *F*2-region independent of geomagnetic activity, *Ann. Geophys.*, *20*, 511–521, doi:10.5194/angeo-20-511-2002.

Danilov, A. D. (2008), Long-term trends in the relation between daytime and nighttime values of *foF*2, *Ann. Geophys.*, *26*, 1199–1206, doi:10.5194/angeo-26-1199-2008.

Danilov, A. D. (2009a), Critical frequencies of *foF*2 as an indicator of trends in thermospheric dynamics, *J. Atmos. Sol. Terr. Phys.*, *71*, 1430–1440, doi:10.1016/j.jastp.2008.04.001.

Danilov, A. D. (2009b), Scatter of *hmF*2 values as an indicator of trends in thermospheric dynamics, *J. Atmos. Sol. Terr. Phys.*, *71*, 1586–1591, doi:10.1016/j.jastp.2009.03.002.

Danilov, A. D., and A. V. Mikhailov (1999), Spatial and seasonal variations of *foF*2 long-term trend, *Ann. Geophys.*, *17*, 1239–1243, doi:10.1007/s00585-999-1239-2.

Danilov, A. D., and L. B. Vanina-Dart (2010), Parameters of the ionospheric *F*2 layer as a source of information on trends in thermospheric dynamics, *Geomagn. Aeron.*, *50*, 187–200, doi:10.1134/S0016793210020064.

Elias, A. G. (2009), Trends in the *F*2 ionospheric layer due to long-term variations in the Earth's magnetic field, *J. Atmos. Sol. Terr. Phys.*, *71*, 1602–1609, doi:10.1016/j.jastp.2009.05.014.

Emmert, J. T., J. M. Picone, J. L. Lean, and S. H. Knowles (2004), Global change in the thermosphere: Compelling evidence of a secular decrease in density, *J. Geophys. Res.*, *109*, A02301, doi:10.1029/2003JA010176.

Emmert, J. T., J. M. Picone, and R. R. Meier (2008), Thermospheric global average density trends 1967–2007, derived from orbits of 5000 near-Earth objects, *Geophys. Res. Lett.*, *35*, L05101, doi:10.1029/2007GL032809.

Emmert, J. T., J. L. Lean, and J. M. Picone (2010), Record-low thermospheric density during the 2008 solar minimum, *Geophys. Res. Lett.*, *37*, L12102, doi:10.1029/2010GL043671.

Fernando, R. P., and I. W. M. Smith (1979), Vibrational relaxation of NO by atomic oxygen, *Chem. Phys. Lett.*, *66*, 218–222, doi:10.1016/0009-2614(79)85002-2.

Fomichev, V. I., A. I. Jonsson, J. de Grandpré, S. R. Beagley, C. McLandress, K. Semeniuk, and T. G. Shepherd (2007), Response of the middle atmosphere to CO_2 doubling: Results from the Canadian Middle Atmosphere Model, *J. Clim.*, *20*, 1121–1144, doi:10.1175/JCLI4030.1.

Garcia, R. R., D. R. Marsh, D. E. Kinnison, B. A. Boville, and F. Sassi (2007), Simulation of secular trends in the middle atmosphere, 1950–2003, *J. Geophys. Res.*, *112*, D09301, doi:10.1029/2006JD007485.

Gavrilov, N. M., S. Fukao, T. Nakamura, C. Jacobi, D. Kürschner, A. H. Manson, and C. E. Meek (2002), Comparative study of interannual changes of the mean winds and gravity wave activity in the middle atmosphere over Japan, central Europe and Canada, *J. Atmos. Sol. Terr. Phys.*, *64*, 1003–1010, doi:10.1016/S1364-6826(02)00055-X.

Glänzer, K., and J. Troe (1975), Vibrational relaxation of NO in collisions with atomic oxygen and chlorine, *J. Chem. Phys.*, *63*, 4352–4357, doi:10.1063/1.431151.

Golitsyn, G. S., A. I. Semenov, and N. N. Shefov (2000), Seasonal variations of the long-term temperature trend in the mesopause region, *Geomagn. Aeron.*, *40*, 198–200.

Gruzdev, A. N., and G. P. Brasseur (2005), Long-term changes in the mesosphere calculated by a two-dimensional model, *J. Geophys. Res.*, *110*, D03304, doi:10.1029/2003JD004410.

Harris, N. R. P., et al. (2008), Ozone trends at northern mid and high latitudes—A European perspective, *Ann. Geophys.*, *26*, 1207–1220, doi:10.5194/angeo-26-1207-2008.

Hoffmann, P., E. Becker, M. Rapp, J. Bremer, W. Singer, and M. Placke (2010), Seasonal and interannual variation of mesospheric waves at middle and high latitudes, paper presented at 6th IAGA/ICMA/CAWSES-II Workshop "Long Term Changes and Trends in the Atmosphere," High Altitude Obs., Natl. Cent. for Atmos. Res., Boulder, Colo.

Holt, J. M., and S. R. Zhang (2008), Long-term temperature trends in the ionosphere above Millstone Hill, *Geophys. Res. Lett.*, *35*, L05813, doi:10.1029/2007GL031148.

Intergovernmental Panel on Climate Change (IPCC) (2007), *Climate Change 2007: The Physical Science Basis: Working Group I Contribution to the Fourth Assessment Report of the IPCC*, edited by S. Solomon et al., Cambridge Univ. Press, New York.

Jacobi, C., R. Schminder, D. Kürschner, J. Bremer, K. M. Greisiger, P. Hoffmann, and W. Singer (1997), Long-term trends in the mesopause wind field obtained from D1 LF wind measurements at Collm, Germany, *Adv. Space Res.*, *20*, 2085–2088, doi:10.1016/S0273-1177(97)00599-1.

Jacobi, C., N. M. Gavrilov, D. Kürschner, and K. Frőhlich (2006), Gravity wave climatology and trends in the mesosphere/lower thermosphere region deduced from low-frequency drift measurements 1984–2003 (52.1°N, 13.2°E), *J. Atmos. Sol. Terr. Phys.*, *68*, 1913–1923, doi:10.1016/j.jastp.2005.12.007.

Jacobi, C., P. Hoffmann, and D. Kürschner (2008), Trends in MLT region winds and planetary waves, Collm (52°N, 15°E), *Ann. Geophys.*, *26*, 1221–1232, doi:10.5194/angeo-26-1221-2008.

Jacobi, C., P. Hoffmann, R. Q. Liu, P. Križan, J. Laštovička, E. G. Merzlyakov, T. V. Solovjova, and Y. I. Portnyagin (2009), Midlatitude mesopause region winds and wave sand comparison with stratospheric variability, *J. Atmos. Sol. Terr. Phys.*, *71*, 1540–1546, doi:10.1016/j.jastp.2009.05.004.

Keating, G. M., R. H. Tolson, and M. S. Bradford (2000), Evidence of long-term global decline in the Earth's thermospheric densities apparently related to anthropogenic effects, *Geophys. Res. Lett.*, *27*, 1523–1526, doi:10.1029/2000GL003771.

Kirkwood, S., P. Dalin, and A. Réchou (2008), Noctilucent clouds observed from the UK and Denmark—Trends and variations over 43 years, *Ann. Geophys.*, *26*, 1243–1254, doi:10.5194/angeo-26-1243-2008.

Klein, F. S., and J. T. Herron (1964), Mass-spectrometric study of the reactions of O atmos with NO and NO_2, *J. Chem. Phys.*, *41*, 1285–1290, doi:10.1063/1.1726061.

Laštovička, J. (2005), On the role of solar and geomagnetic activity in long-term trends in the atmosphere-ionosphere system, *J. Atmos. Sol. Terr. Phys.*, *67*, 83–92, doi:10.1016/j.jastp.2004.07.019.

Laštovička, J. (2009), Global pattern of trends in the upper atmosphere and ionosphere: Recent progress, *J. Atmos. Sol. Terr. Phys.*, *71*, 1514–1528, doi:10.1016/j.jastp.2009.01.010.

Laštovička, J., and J. Bremer (2004), An overview of long-term trends in the lower ionosphere below 120 km, *Surv. Geophys.*, *25*, 69–99, doi:10.1023/B:GEOP.0000015388.75164.e2.

Laštovička, J., and D. Pancheva (1991), Changes in characteristics of planetary waves at 80–100 km over central and southern Europe since 1980, *Adv. Space Res.*, *11*, 31–34, doi:10.1016/0273-1177(91)90399-5.

Laštovička, J., R. A. Akmaev, G. Beig, J. Bremer, and J. T. Emmert (2006a), Global change in the upper atmosphere, *Science*, *314*, 1253–1254, doi:10.1126/science.1135134.

Laštovička, J., et al. (2006b), Long-term trends in *foF*2: A comparison of various methods, *J. Atmos. Sol. Terr. Phys.*, *68*, 1854–1870, doi:10.1016/j.jastp.2006.02.009.

Laštovička, J., R. A. Akmaev, G. Beig, J. Bremer, J. T. Emmert, C. Jacobi, M. J. Jarvis, G. Nedoluha, Y. I. Portnyagin, and T. Ulich (2008a), Emerging pattern of global change in the upper atmosphere and ionosphere, *Ann. Geophys.*, *26*, 1255–1268, doi:10.5194/angeo-26-1255-2008. (Available at www.ann-geophys.net/26/1255/2008/.)

Laštovička, J., X. Yue, and W. Wan (2008b), Long-term trends in *foF*2: Their estimating and origin, *Ann. Geophys.*, *26*, 593–598, doi:10.5194/angeo-26-593-2008.

Laštovička, J., P. Križan, and M. Kozubek (2010), Long-term trends in the middle atmosphere dynamics at northern middle latitudes—One regime or two different regimes?, *Atmos. Chem. Phys. Discuss.*, *10*, 2633–2668, doi:10.5194/acpd-10-2633-2010. (Available at www.atmos-chem-phys-discuss.net/10/2633/2010/.)

Lübken, F. J. (2001), No long term change of the thermal structure in the mesosphere at high latitudes during summer, *Adv. Space Res.*, *28*, 947–953, doi:10.1016/S0273-1177(01)80022-3.

Lübken, F.-J., U. Berger, and G. Baumgartner (2009), Stratospheric and solar cycle effects on long-term variability of mesospheric ice clouds, *J. Geophys. Res.*, *114*, D00I06, doi:10.1029/2009JD012377.

Lübken, F.-J., U. Berger, J. Fiedler, G. Baumgartner, and M. Gerding (2010), Trends and solar cycle effects in mesospheric ice clouds, paper presented at 38th Scientific Assembly, Comm. on Space Res., Bremen, Germany.

Marcos, F. A., J. O. Wise, M. J. Kendra, N. J. Grossbard, and B. R. Bowman (2005), Detection of a long-term decrease in thermospheric neutral density, *Geophys. Res. Lett.*, *32*, L04103, doi:10.1029/2004GL021269.

Merzlyakov, E., C. Jacobi, Y. I. Portnyagin, and T. V. Solovjova (2009), Structural changes in trend parameters of the MLT winds based on wind measurements at Obninsk (55°N, 37°E) and Collm (52°N, 15°E), *J. Atmos. Sol. Terr. Phys.*, *71*, 1547–1557, doi:10.1016/j.jastp.2009.05.013.

Mikhailov, A. V. (2002), The geomagnetic control concept of the *F*2-layer parameter long-term trends, *Phys. Chem. Earth*, *27*, 595–606.

Mikhailov, A. V. (2006), Ionospheric long-term trends: Can the geomagnetic control and the greenhouse hypothesis be reconciled?, *Ann. Geophys.*, *24*, 2533–2541, doi:10.5194/angeo-24-2533-2006.

Mikhailov, A. V., and B. A. de la Morena (2003), Long-term trends of f_oE and geomagnetic activity variations, *Ann. Geophys.*, *21*, 751–760, doi:10.5194/angeo-21-751-2003.

Mikhailov, A. V., and D. Marin (2000), Geomagnetic control of the *foF*2 long-term trends, *Ann. Geophys.*, *18*, 653–665, doi:10.1007/s00585-000-0653-2.

Mikhailov, A. V., and D. Marin (2001), An interpretation of the *foF*2 and *hmF*2 long-term trends in the framework of the geomagnetic control concept, *Ann. Geophys.*, *19*, 733–748, doi:10.5194/angeo-19-733-2001.

Mikhailov, A. V., D. Marin, T. Y. Leschinskaya, and M. Herraiz (2002), A revised approach to *foF*2 long-term trend analysis, *Ann. Geophys.*, *20*, 1663–1675, doi:10.5194/angeo-20-1663-2002.

Mlynczak, M., L. Hunt, and J. Mast (2010), Observations of natural variability in the mesosphere-thermosphere climate system from the TIMED/SABER instrument—And a view to the future, paper presented at 6th IAGA/ICMA/CAWSES-II Workshop "Long Term Changes and Trends in the Atmosphere," High Altitude Obs., Natl. Cent. for Atmos. Res., Boulder, Colo.

Mursula, K., and D. Martini (2006), Centennial increase in geomagnetic activity: Latitudinal difference and global estimates, *J. Geophys. Res.*, *111*, A08209, doi:10.1029/2005JA011549.

Nielsen, K. P., F. Sigernes, E. Raustein, and C. S. Deehr (2002), The 20-year change of the Svalbard OH-temperatures, *Phys. Chem. Earth*, *27*, 555–561.

Nossal, S. M., E. J. Mierkiewicz, F. L. Roesler, L. M. Haffner, R. J. Reynolds, and R. C. Woodward (2008), Geocoronal hydrogen observations spanning three solar minima, *J. Geophys. Res.*, *113*, A11307, doi:10.1029/2008JA013380.

Oltmans, S. J., H. Vömel, D. J. Hofmann, K. H. Rosenlof, and D. Kley (2000), The increase in stratospheric water vapor from balloonborne, frostpoint hygrometer measurements at Washington, D.C., and Boulder, Colorado, *Geophys. Res. Lett.*, *27*, 3453–3456, doi:10.1029/2000GL012133.

Pollock, D. S., G. B. I. Scott, and L. F. Phillips (1993), Rate constant for quenching of $CO_2(010)$ by atomic oxygen, *Geophys. Res. Lett.*, *20*, 727–730, doi:10.1029/93GL01016.

Portnyagin, Y. I., E. G. Merzlyakov, T. V. Solovjova, C. Jacobi, D. Kürschner, A. Manson, and C. Meek (2006), Long-term trends and year-to-year variability of mid-latitude mesosphere/lower thermosphere winds, *J. Atmos. Sol. Terr. Phys.*, *68*, 1890–1901, doi:10.1016/j.jastp.2006.04.004.

Qian, L., R. G. Roble, S. C. Solomon, and T. J. Kane (2006), Calculated and observed climate change in the thermosphere, and a prediction for solar cycle 24, *Geophys. Res. Lett.*, *33*, L23705, doi:10.1029/2006GL027185.

Qian, L., S. C. Solomon, R. G. Roble, and T. J. Kane (2008), Model simulations of global change in the ionosphere, *Geophys. Res. Lett.*, *35*, L07811, doi:10.1029/2007GL033156.

Qian, L., A. G. Burns, S. C. Solomon, and R. G. Roble (2009), The effect of carbon dioxide cooling on trends in the *F*2-layer ionosphere, *J. Atmos. Sol. Terr. Phys.*, *71*, 1592–1601, doi:10.1016/j.jastp.2009.03.006.

Randel, W. J., F. Wu, H. Vömel, G. E. Nedoluha, and P. Forster (2006), Decreases in stratospheric water vapor after 2001: Links to changes in the tropical tropopause and the Brewer-Dobson circulation, *J. Geophys. Res.*, *111*, D12312, doi:10.1029/2005JD006744.

Remsberg, E. E. (2009), Trends and solar cycle effects in temperatures versus altitude from the Halogen Occultation Experiment for the mesosphere and upper stratosphere, *J. Geophys. Res.*, *114*, D12303, doi:10.1029/2009JD011897.

Richmond, A. D., E. C. Ridley, and R. G. Roble (1992), A thermosphere/ionosphere general circulation model with coupled electrodynamics, *Geophys. Res. Lett.*, *19*, 601–604, doi:10.1029/92GL00401.

Rishbeth, H. (1990), A greenhouse effect in the ionosphere?, *Planet. Space Sci.*, *38*, 945–948, doi:10.1016/0032-0633(90)90061-T.

Rishbeth, H. (1998), How the thermospheric circulation affects the ionospheric *F*2 layer, *J. Atmos. Sol. Terr. Phys.*, *60*, 1385–1402, doi:10.1016/S1364-6826(98)00062-5.

Rishbeth, H., and R. G. Roble (1992), Cooling of the upper atmosphere by enhanced greenhouse gases: Modelling of thermospheric and ionospheric effects, *Planet. Space Sci.*, *40*, 1011–1026, doi:10.1016/0032-0633(92)90141-A.

Roble, R. G., and R. E. Dickinson (1989), How will changes in carbon dioxide and methane modify the mean structure of the mesosphere and lower thermosphere?, *Geophys. Res. Lett.*, *16*, 1441–1444, doi:10.1029/GL016i012p01441.

Roble, R. G., and E. C. Ridley (1994), Thermosphere-ionosphere-mesosphere-electrodynamics general circulation model (TIME-GCM): Equinox solar min simulations, 30–500 km, *Geophys. Res. Lett.*, *21*, 417–420, doi:10.1029/93GL03391.

Rodgers, C. D., F. W. Taylor, A. H. Muggeridge, M. Lopez-Puertas, and M. A. Lopea-Valverde (1992), Local thermodynamic equilibrium of carbon dioxide in the upper atmosphere, *Geophys. Res. Lett.*, *19*, 589–592, doi:10.1029/92GL00160.

Scherer, M., H. Vömel, S. Fueglistaler, S. J. Oltmans, and J. Staehelin (2008), Trends and variability of midlatitude stratospheric water vapour deduced from the re-evaluated Boulder balloon series and HALOE, *Atmos. Chem. Phys.*, *8*, 1391–1402, doi:10.5194/acp-8-1391-2008.

Schmidt, H., G. P. Brasseur, M. Charron, E. Manzini, M. A. Giorgetta, T. Diehl, V. I. Fomichev, D. Kinnison, D. Marsh, and S. Walters (2006), The HAMMONIA chemistry climate model: Sensitivity of the mesopause region to the 11-year solar cycle and CO_2 doubling, *J. Clim.*, *19*, 3903–3931, doi:10.1175/JCLI3829.1.

Schwarzkopf, M. D., and V. Ramaswamy (2008), Evolution of stratospheric temperature in the 20th century, *Geophys. Res. Lett.*, *35*, L03705, doi:10.1029/2007GL032489.

Semenov, A. I., N. N. Shefov, E. V. Lysenko, G. V. Givishvili, and A. V. Tikhonov (2002), The seasonal peculiarities of behavior of the long-term temperature trends in the middle atmosphere at the mid-latitudes, *Phys. Chem. Earth*, *27*, 529–534.

Sharma, R. D., and R. G. Roble (2002), Cooling mechanisms of the planetary thermospheres: The key role of O atom vibrational excitation of CO_2 and NO, *ChemPhysChem*, *3*(10), 841−843.

Sharma, R. D., and P. P. Wintersteiner (1990), Role of carbon dioxide in cooling planetary atmospheres, *Geophys. Res. Lett.*, *17*, 2201–2204, doi:10.1029/GL017i012p02201.

She, C.-Y., D. A. Krueger, R. Akmaev, H. Schmidt, E. Talaat, and S. Yee (2009), Long-term variability in mesopause region temperatures over Fort Collins, Colorado (41°N, 105°W) based on lidar observations from 1990 through 2007, *J. Atmos. Sol. Terr. Phys.*, *71*, 1558–1564, doi:10.1016/j.jastp.2009.05.007.

Shettle, P. E., M. T. DeLand, G. E. Thomas, and J. J. Olivero (2009), Long term variations in the frequency of polar mesospheric clouds in the Northern Hemisphere from SBUV, *Geophys. Res. Lett.*, *36*, L02803, doi:10.1029/2008GL036048.

Shved, G. M., L. E. Khvorostovskaya, I. Y. Potekhim, A. I. Demyanikov, A. A. Kutepov, and V. I. Fomichev (1991), Measurement of the quenching rate constant for collisions $CO_2(01^10)$–O: The importance of the rate constant magnitude for the thermal regime and radiation of the lower thermosphere, *Izv. Akad. Nauk SSSR, Ser. Fiz.*, *27*, 431–437.

Smirnova, M., E. Belova, S. Kirkwood, and N. Mitchell (2010), Polar mesosphere summer echoes with ESRAD, Kiruna, Sweden: Variations and trends over 1997–2008, *J. Atmos. Sol. Terr. Phys.*, *72*, 435–447, doi:10.1016/j.jastp.2009.12.014.

Solomon, S., K. H. Rosenlof, R. W. Portmann, J. S. Daniel, S. M. Davis, T. J. Sanford, and G.-K. Plattner (2010a), Contribution of stratospheric water vapor to decadal changes in the rate of global warming, *Science*, *327*, 1219–1223, doi:10.1126/science.1182488.

Solomon, S. C., T. N. Woods, L. V. Didkovsky, J. T. Emmert, and L. Qian (2010b), Anomalously low solar extreme-ultraviolet irradiance and thermospheric density during solar minimum, *Geophys. Res. Lett.*, *37*, L16103, doi:10.1029/2010GL044468.

Sridharan, S., T. Tsuda, and S. Gurubaran (2010), Long-term tendencies in the mesosphere/lower thermosphere mean winds and tides observed by medium frequency radar at Tirunaveli (8.7°N, 77.8°E), *J. Geophys. Res.*, *115*, D08109, doi:10.1029/2008JD011609.

Stiller, G. P., et al. (2008), Global stratospheric water vapour distributions from MIPAS/Envisat for the period 2002 to 2008, paper presented at 4th General Assembly, Stratospheric Processes and Their Role in Clim., Bologna, Italy, 31 August to 5 September.

Venkat Ratnam, M., A. K. Patra, and B. V. Krishna Murthy (2010), Tropical mesopause: Is it always close to 100 km?, *J. Geophys. Res.*, *115*, D06106, doi:10.1029/2009JD012531.

Yue, X., W. Wan, L. Liu, B. Ning, and B. Zhao (2006), Applying artificial neural network to derive long-term *foF*2 trends in the Asia/Pacific sector from ionosonde observations, *J. Geophys. Res.*, *111*, A10303, doi:10.1029/2005JA011577.

Yue, X., L. Liu, W. Wan, Y. Wei, and Z. Ren (2008), Modeling the effects of secular variation of geomagnetic field orientation on the ionospheric long term trend over the past century, *J. Geophys. Res.*, *113*, A10301, doi:10.1029/2007JA012995.

Zhang, S.-R., and J. M. Holt (2011), Millstone Hill ISR observations of upper atmospheric long-term changes: Height dependency, *J. Geophys. Res.*, doi:10.1029/2010JA016414, in press.

J. Laštovička, Institute of Atmospheric Physics, ASCR, Bocni II, 14131 Prague, Czech Republic.

L. Qian, R. G. Roble, and S. C. Solomon, High Altitude Observatory, National Center for Atmospheric Research, 3080 Center Green Dr., Boulder, CO 80301, USA. (lquian@ucar.edu)